NASA TECHNICAL NOTE

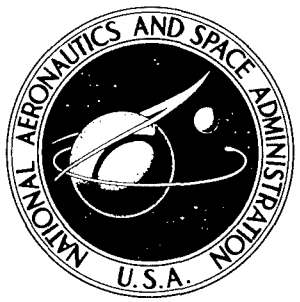

NASA TN D-3059

NASA TN D-3059

LANDING CHARACTERISTICS OF THE APOLLO SPACECRAFT WITH DEPLOYED-HEAT-SHIELD IMPACT ATTENUATION SYSTEMS

by Sandy M. Stubbs

Langley Research Center
Langley Station, Hampton, Va.

NATIONAL AERONAUTICS AND SPACE ADMINISTRATION • WASHINGTON, D. C. • JANUARY 1966

NASA TN D-3059

LANDING CHARACTERISTICS OF THE APOLLO SPACECRAFT WITH DEPLOYED-HEAT-SHIELD IMPACT ATTENUATION SYSTEMS

By Sandy M. Stubbs

Langley Research Center
Langley Station, Hampton, Va.

Technical Film Supplement L-886 available on request.

NATIONAL AERONAUTICS AND SPACE ADMINISTRATION

For sale by the Clearinghouse for Federal Scientific and Technical Information
Springfield, Virginia 22151 – Price $3.00

LANDING CHARACTERISTICS OF THE APOLLO SPACECRAFT WITH DEPLOYED-HEAT-SHIELD IMPACT ATTENUATION SYSTEMS

By Sandy M. Stubbs
Langley Research Center

SUMMARY

An experimental investigation was made to determine the landing characteristics of a 1/4-scale dynamic model of the Apollo spacecraft command module using two different active (heat shield deployed prior to landing) landing systems for impact attenuation. One landing system (configuration 1) consisted of six hydraulic struts and eight crushable honeycomb struts. The other landing system (configuration 2), consisting of four hydraulic struts and six strain straps, was lighter. Tests made on water and the hard clay-gravel composite landing surfaces simulated parachute letdown (vertical) velocities of 23 ft/sec (7.0 m/s) (full scale). Landings made on the sand landing surface simulated vertical velocities of 30 ft/sec (9.1 m/s). Horizontal velocities of from 0 to 50 ft/sec (15 m/s) were simulated. Landing attitudes ranged from -30° to 20°, and the roll attitudes were 0°, 90°, and 180°.

For configuration 1, maximum normal accelerations at the vehicle center of gravity for landings on water, sand, and the hard clay-gravel composite surface were 9g, 20g, and 18g, respectively. The maximum normal center-of-gravity acceleration for configuration 2 which was landed only on the hard clay-gravel landing surface was approximately 19g. Accelerations for configuration 2 were generally equal to or lower than accelerations for configuration 1 and normal and longitudinal accelerations for both configurations were considered to be below human acceleration tolerance limits without using crew-couch shock absorbers or other load alleviation devices.

Configuration 1 was stable for all landings made on calm water. It was stable on the sand landing surface for landing attitudes from -20° to 5° for the 0° roll landing condition. For landings on a hard clay-gravel composite landing surface, both configurations at 0° roll had a stable region between two unstable regions, the most desirable landing attitude being about -10°. The stability envelopes for configuration 1 were generally slightly larger than those for configuration 2 and stability characteristics for both configurations indicate that roll control of the spacecraft would be desirable. Configuration 1 was tested for flotation stability and it was found to be stable in an approximately upright attitude. The vehicle in a turned-over condition was righted by waves 2 feet (0.61 m) high and 36 feet (11 m) long (full scale).

INTRODUCTION

One of the many aspects of manned space flight being investigated by the National Aeronautics and Space Administration is the landing of a spacecraft upon its return to earth. Landing characteristics of various models of manned spacecraft are presented in references 1 to 5. The Apollo command module is currently being developed for a three-man lunar mission which includes an earth landing by parachute.

It is desirable that an earth-environment landing system have the capability of landing on firm soil as well as on water. Passive landing systems (landing systems that do not require heat-shield deployment or braking rockets) when landed on firm soil can easily result in impact accelerations that exceed human acceleration-tolerance levels; thus, this type of landing system is relegated to a water landing. If the requirement of a soil-landing capability is to be met, it is probably necessary that an active landing system be used.

In the present investigation, two different active landing systems in which the heat shield is deployed have been tested by using a 1/4-scale dynamic model. The first configuration was designed and constructed to be used as a landing system for the Apollo command module. (See ref. 6.) It consisted of six vertically oriented hydraulic struts and eight horizontally oriented honeycomb struts. In an attempt to obtain a lightweight landing system that would give landing characteristics comparable with this configuration, several types of struts, number of struts, and arrangements were tested before a suitable configuration evolved. This second configuration consisted of four vertical struts and six lightweight strain straps. Both configurations depend on the heat shield being strong enough to transmit the impact loads to the shock strut system.

The purpose of the present investigation is to determine the accelerations and landing characteristics of a spacecraft with two different active landing systems. Tests were made on water, sand, and a hard clay-gravel composite landing surface for various vertical velocities, horizontal velocities, and landing attitudes simulating parachute letdown. The investigation was conducted in the Langley impacting structures facility.

The units used for the physical quantities defined in this paper are given both in U.S. Customary Units and in the International System of Units (SI). (See ref. 7.) Appendix A presents factors relating these two systems of units.

DESCRIPTION OF MODEL

The model used in the investigation was a 1/4-scale dynamic model of the command module of the Apollo spacecraft. Detailed information of the model construction is given in reference 6 and model dimensions are given in figure 1. The model was constructed

of an aluminum frame to which an outer skin of approximately 1/8 in. (0.635 cm) (model scale) thick fiber glass and plastic was attached. The bottom of the crew compartment was filled with balsa wood to reduce structural vibrations. Mahogany blocks were inserted in the balsa wood to serve as accelerometer mounts. The scale relationships used in the investigation are shown in table I. The basic model was used with two different active landing systems.

Configuration 1

Configuration 1 consisted of the basic model having a mass of 3.56 slugs (51.95 kg) and a landing system composed of six vertical hydraulic struts and eight horizontal struts. The pertinent parameters of the spacecraft are given in table II and the locations of the struts are shown in figure 2. Photographs of configuration 1 are shown in figure 3. Photographs of the assembled and disassembled struts are shown in figure 4. Details of the development of both struts are reported in reference 6. The vertical hydraulic strut used a mixture of 80-percent ethylene glycol and 20-percent water as the working fluid with a 0.5-percent wetting agent added by mass to facilitate the release of entrained air bubbles. The hydraulic strut used on configuration 1 employed a tapered metering pin and an orifice of 0.187 in. (0.475 cm) (model scale) diameter. The force characteristics of a single dynamically loaded vertical strut are shown in figure 5. To obtain the typical force-time curve shown, an accelerometer was mounted on a 0.89 slug (12.98 kg) lead mass (representing one-fourth of the mass of the model) and dropped so that the velocity at impact with the hydraulic strut was 15 ft/sec (4.6 m/s) (model scale). The maximum force developed by the hydraulic strut was approximately 520 lbf (2310 N) (model scale).

The horizontal struts were double-acting struts using aluminum honeycomb as a crushing shock absorber. The struts were designed to crush the honeycomb whether in tension or compression and were so located that at least four horizontal struts would be acting for all landings (two in compression and two in tension). The aluminum honeycomb used in the horizontal struts was MIL 111-A 1/4-3003-0.001 P aluminum honeycomb. The force characteristics of the honeycomb used in each horizontal strut are shown in figure 6. To obtain the typical force-time curve shown, an accelerometer was mounted on a 0.89 slug (12.98 kg) lead mass (representing one-fourth of the mass of the model) and dropped so that the velocity at impact with the honeycomb was 4.4 ft/sec (1.3 m/s) model scale. The maximum force developed by the honeycomb was approximately 370 lbf (1650 N).

Configuration 2

Configuration 2 consisted of the basic model having a mass of 4.36 slugs (63.6 kg) and a landing system composed of four vertical hydraulic struts and six horizontal strain

straps. The pertinent parameters of the spacecraft are given in table II and the locations of the struts and strain straps are shown in figure 7. The mass of configuration 2 differed from configuration 1 because of an attempt, during the test program, to keep abreast of prototype mass estimate changes. Photographs of configuration 2 are shown in figure 8. The vertical strut was the same as that used on configuration 1 with the exception that the orifice diameter through which the metering pin operates was 0.185 in. (0.470 cm) (model scale). The force characteristics for the vertical strut used with configuration 2 are shown in figure 9. To obtain the typical force-time curve shown, an accelerometer was mounted on a 1.24 slug (18.1 kg) lead mass (representing slightly more than one-fourth of the mass of the model) and dropped so that the velocity at impact with the hydraulic strut was 15 ft/sec (4.6 m/s) (model scale). The maximum force developed by the hydraulic strut was approximately 780 lbf (3469 N) model scale. The increase in force produced by this strut was necessary to stop the increased mass of configuration 2.

The horizontal strain straps used on configuration 2 are shown in figure 10. The strain straps were made of low-carbon nickel metal wire. The stress-strain characteristics of the metal are shown in figure 11. By using a yield stress of approximately 30,000 lbf/in^2 (207 MN/m^2), the front straps (by using four wires of 0.08 in. (0.20 cm) diameter) (see fig. 7) were designed to yield at a force of about 600 lbf (2670 N); the side straps (three wires), at a force of 450 lbf (2000 N); and the rear straps (two wires), at a force of 300 lbf (1330 N) (model scale). Several other arrangements of strain straps, restraint cables, honeycomb, and balsa-wood shock absorbers, were tested before arriving at the landing system presented for configuration 2. The basic criterion considered in determining the configuration 2 landing system was that it offers a lower mass impact attenuation system that could be used to land the vehicle without major compromises in the landing characteristics (impact load g and stability). A mass comparison for the two landing systems is presented in appendix B. The mass determined for configuration 2 is based on using nickel strain straps; however, on the full-scale vehicle, titanium might be used for a further weight reduction since it possesses a better stress-density ratio than nickel and has adequate temperature and ductility qualities.

Heat-Shield Structure

The heat shields used on configurations 1 and 2 were constructed of two layers of fiber glass separated by a layer of plastic foam. Construction details are presented in reference 6. Load deflection characteristics were obtained on the heat shields by using the apparatus shown in figure 12. Load-deflection curves are presented in figure 13. The deflection of the heat shield at impact is relatively small compared with the stroke of approximately 3 in. (8 cm) provided by the vertical hydraulic strut.

APPARATUS AND PROCEDURE

Test Conditions

Configuration 1 was landed on water, sand, and hard clay-gravel composite landing surfaces whereas configuration 2 was landed only on the hard clay-gravel composite landing surface. Tests made on water and the hard clay-gravel composite landing surfaces simulated parachute letdown (vertical) velocities of 23 ft/sec (7.0 m/s) (full scale). Landings made on the sand landing surface simulated vertical velocities of 30 ft/sec (9.1 m/s). Horizontal velocities of from 0 to 50 ft/sec (15 m/s) were simulated. Landing attitudes ranged from -30° to 20°, and roll attitudes were 0°, 90°, and 180°. Figure 14 shows the model acceleration axes, flight path, force directions, and landing attitudes. It should be noted that the roll and yaw attitudes for landing are different from the standard aircraft axes.

The water landing tests were made in calm fresh water. The sand used for the sand landings was dry Standard Ottawa testing sand. It was not meant to represent any particular terrain but was chosen because its controlled uniform characteristics favor reproducible experiments. The composite material used for the hard surface landings was a clay-gravel mixture that was moistened and rolled smooth as it was being installed. After rolling it smooth, it was allowed to dry to a hard surface before testing began. Repairs were made occasionally as the surface would loosen during repeated or severe impacts. The coefficient of sliding friction between the fiber-glass heat shield and the clay-gravel composite surface was approximately 0.35. The drag force for sand landings was not determined because it varies with varying depth of penetration.

It was assumed that the spacecraft would be hung under the parachute at a -10° attitude. This assumption is based on results presented in reference 8 that indicate negative landing attitudes are more stable than positive attitudes for landings at 0° roll on land. A variation in landing attitude from -30° to 20° was tested to simulate the swing of the spacecraft about the -10° attitude under the letdown parachutes. Most of the tests were conducted at 0° roll and 0° yaw; however, a limited number of tests were conducted at 90° and 180° roll and at yaw angles from 0° to 14°.

Instrumentation

Normal, longitudinal, and transverse accelerations were measured at the center of gravity of the vehicle and normal and longitudinal accelerations were measured at the center of gravity of the crew couch (see fig. 1) by using linear strain-gage-type accelerometers. Angular (pitch) accelerations were measured with matched pairs of linear accelerometers suitably connected electrically. Signals from the accelerometers were transmitted through trailing cables to the recording equipment. The response

characteristics of the accelerometers and related recording equipment (control box, oscillograph, and galvanometers) are given in table III.

Launch Procedure and Apparatus

A sketch showing the launch procedure is given in figure 15. A pendulum was released from a predetermined height to produce the desired horizontal velocity. At the end of one-quarter period, the model was released and the free fall gave the desired vertical velocity. Photographs of the launch apparatus and two of the landing surfaces are shown in figure 16. Motion pictures were made to record the landing behavior of the model.

Flotation tests were made by using an oscillating-type wave maker to produce a train of waves 2 ft (0.61 m) high by 36 ft (11 m) long (full scale) for flotation stability investigations. During the flotation tests, the heat shield was restrained only by the landing system which allowed it to open or close depending on the flotation position of the spacecraft.

RESULTS AND DISCUSSION

All the data obtained in the investigation are presented in tabular form in tables IV and V but only selected conditions, in general those that have quantities of data and show definite trends, are plotted and discussed. For example, acceleration data at the 0^{o} roll angle only are plotted and discussed, and for water landings only the data obtained at the 23 ft/sec (7.0 m/s) vertical velocity are plotted and discussed. All the values presented in this section are full scale unless otherwise indicated.

A motion-picture film supplement showing landing tests of the 1/4-scale model of the Apollo command module made on water, sand, and hard clay-gravel composite landing surfaces has been prepared and is available on loan. A request card form will be found at the back of this paper.

Landing Acceleration

Configuration 1.- Typical oscillograph records obtained from landings of configuration 1 on water, sand, and hard clay-gravel composite landing surfaces are shown in figure 17. Figure 17(a) is an oscillograph record of a landing made on calm water at a vertical velocity of 23 ft/sec (7.0 m/s); figure 17(b) is a landing made on a flat sand landing surface at a vertical velocity of 30 ft/sec (9.1 m/s); and figure 17(c) is a landing made on a clay-gravel composite landing surface at a vertical velocity of 23 ft/sec (7.0 m/s). The dashed lines are fairings of the accelerometer traces. Maximum

acceleration data presented in figure 18 and in tables IV and V were obtained from similar fairings.

Water landing surface: Maximum acceleration data for configuration 1 when landed on a calm water landing surface are shown in figure 18(a). The maximum normal acceleration at the center of gravity was 9g. The longitudinal acceleration data occasionally contained both positive and negative values. Generally, when positive and negative values are plotted at the same landing attitude, they were obtained from the same landing. The longitudinal accelerations ranged from 8g to -8.5g. The angular accelerations ranged from 70 rad/sec^2 to -50 rad/sec^2. Maximum normal acceleration at the crew-couch center of gravity was 10g.

Sand landing surface: Maximum acceleration data for configuration 1, when landed on a flat sand landing surface are shown in figure 18(b). It should be noted that landings made on the sand landing surface had a higher vertical velocity than landings made on water or on the hard clay-gravel composite surface. The shaded symbols indicate that the vehicle turned over. The data presented are for the initial impact and not for the impacts resulting from tumbling. When turnover occurred, higher accelerations were recorded during the tumbling action. Accelerations at turnover are not of interest in this report because the model structure impacting the landing surface during turnover is not representative of the spacecraft structure.

Maximum normal acceleration at the spacecraft center of gravity was 20g whereas maximum normal accelerations at the crew couch increased from 14g at a -20° attitude to 35g at a 15° attitude. At the vehicle center of gravity there was no discernible effect of horizontal velocity on normal accelerations; however, at the couch center of gravity, normal acceleration increased with an increase in horizontal velocity for positive landing attitudes.

Longitudinal accelerations at the vehicle center of gravity ranged from 19g to -9g, some conditions giving both positive and negative acceleration values. Maximum longitudinal accelerations at the crew couch were similar to those obtained at the spacecraft center of gravity.

Angular accelerations ranged from 130 rad/sec^2 to -200 rad/sec^2. Most landings at negative landing attitudes had both positive and negative angular accelerations.

Clay-gravel composite landing surface: Maximum acceleration data for configuration 1, when landed on a hard clay-gravel composite surface are shown in figure 18(c). The maximum normal acceleration at the vehicle center of gravity was 18g, the maximum longitudinal acceleration was 18g, and the angular accelerations ranged from about 140 rad/sec^2 to -180 rad/sec^2. The maximum normal accelerations at the crew-couch center of gravity were 32g and -12g.

All landings made with configuration 1 on water, sand, and the hard clay-gravel composite landing surfaces gave accelerations that are considered to be within the human tolerance limits presented in references 9 and 10. These accelerations were obtained without the use of crew-couch shock absorbers or other load-alleviation devices.

Configuration 2.- Typical oscillograph records obtained from landings of configuration 2 on a hard clay-gravel composite surface are shown in figure 19. The records shown are for vertical velocities of approximately 24 ft/sec (7.3 m/s), a horizontal velocity of 30 ft/sec (9.1 m/s), and a roll attitude of 0°. Figure 19(a) is a record for a landing attitude of -11° and figure 19(b) is a record for a landing attitude of -27°. The vehicle turned over at the -27° attitude.

Maximum acceleration data for configuration 2 when landed on a hard clay-gravel composite surface are shown in figure 20. The maximum normal acceleration at the vehicle center of gravity was about 19g and at the crew couch 21.5g. One landing at a horizontal velocity of 40 ft/sec (12.0 m/s) and at an attitude of -4° resulted in the heat shield deforming sufficiently to make contact with the crew compartment (Bottoming). When this condition occurred, the normal acceleration was increased about 45 percent.

The maximum longitudinal acceleration at the spacecraft center of gravity was about 11g and did not vary for a wide range of landing attitudes. The maximum longitudinal accelerations at the crew-couch center of gravity are very similar to the longitudinal accelerations at the spacecraft center of gravity. The strain straps used to attenuate the longitudinal accelerations stretched a maximum of 3 percent of their length.

The angular accelerations for landings made on the hard clay-gravel composite surface ranged from approximately 80 rad/sec^2 to about -130 rad/sec^2. Most conditions tested with configuration 2 had both positive and negative angular accelerations.

Landings with configuration 2 gave accelerations considered to be within human tolerance levels. A comparison between the accelerations of configuration 1 and configuration 2 (figs. 18(c) and 20) indicates that maximum accelerations for configuration 2 were generally the same or lower than maximum accelerations for configuration 1 even though the masses of the two configurations are different.

Landing Stability

Stable landings are defined, for use in this report, as landings in which the vehicle did not turn over. Unstable landings are defined as landings that resulted in turnover. Marginal stability occurred when the vehicle tilted to such an attitude that small changes in friction coefficient might result in turnover. Marginal stability was determined after reviewing motion-picture data from the model tests.

Configuration 1.- Configuration 1 had stable landings for all conditions tested on calm water. (See fig. 21.) Stability characteristics for configuration 1 landed on the dry sand landing surface are shown in figure 22. The shaded symbols indicate turnover and the open or clear symbols indicate test conditions resulting in stable landing characteristics. Open symbols with a line drawn through them indicate test conditions that are marginally stable. Stable landings were made for landing attitudes from -20° to 5°, at a 0° roll attitude, for horizontal velocities up to 50 ft/sec (15 m/s). As the landing attitude is increased from 5° to 20°, the stability characteristics deteriorate through a marginally stable region to an unstable region.

Landing stability for configuration 1 when landed on a hard clay-gravel landing surface are shown in figure 23. The solid data points again indicate turnover. Stability data at the 0° roll attitude (fig. 23(a)) indicate a stable region between two unstable regions, the most desirable landing attitude being approximately -10°. At the high horizontal velocity, 50 ft/sec (15.1 m/s), the stable landing attitudes are from approximately -2° to -16° for a spread of only 14°. This stable landing attitude spread increases as the horizontal velocity decreases until at 20 ft/sec (6.1 m/s), the spread is approximately 23°. There is a limited amount of data at the 90° roll condition (fig. 23(b)) but all the conditions tested were stable. The data at 180° roll (fig. 23(c)) indicate a stable region for a horizontal velocity of 30 ft/sec (9.0 m/s) at landing attitudes from -8° to -1°. This stable region increased with a decrease in horizontal velocity.

Configuration 2.- Landing stability plots for configuration 2 are shown in figure 24 for landings on the hard clay-gravel composite landing surface. Stability at the 0° roll attitude (fig. 24(a)) indicates a stable region between two unstable regions, the most desirable landing attitude being approximately -11°. At the high horizontal velocity, 50 ft/sec (15.1 m/s), the stable landing attitudes are from approximately -7° to -16° for a spread of only 9°. This stable-landing-attitude spread increases as the horizontal velocity decreases until at 20 ft/sec (6.1 m/s), the spread is about 21°. A comparison between the stability characteristics of configuration 1 and configuration 2 for landings at 0° roll (figs. 23(a) and 24(a)), shows configuration 1 to have a slightly larger stable region.

When configuration 2 was landed at a 90° roll attitude and a horizontal velocity of 30 ft/sec (9.0 m/s), the entire range of landing attitudes tested (-27° to 8°) was stable or marginally stable. However, at the 50 ft/sec (15.1 m/s) horizontal velocity, there were no stable landings.

When landed at 180° roll, configuration 2 was stable at a horizontal velocity of 50 ft/sec (15.1 m/s) for attitudes from -2° to the highest positive angle tested. The stable region increased with a decrease in horizontal velocity.

Stability Control

It has been assumed that the spacecraft would be supported from the parachute at a -10° landing attitude and the data presented have shown this to be a desirable landing condition for 0° roll. Nevertheless, there is a distinct possibility that turnover could occur, under certain combinations of effective landing attitude (a combination of parachute swing, roll attitude, and ground slope) and horizontal velocity. The variety of stable regions that have been shown to be available for landings made at roll angles of 0°, 90°, and 180° indicates the desirability of giving the crew some roll control of the spacecraft. With roll control and a knowledge of the horizontal velocity, the crew could choose a landing condition that would increase the probability of a stable landing.

Flotation

The brief flotation investigation conducted with configuration 1 indicated two stable flotation positions for the vehicle when floated in calm water. The vehicle was stable in an approximately upright position (fig. 25(a)) and in a turned-over position (fig. 25(b)). When waves 2 ft (0.61 m) high and 36 ft (11 m) long were introduced, the vehicle in the turned-over condition would quickly right itself. It was found that a force of 64 lbf (285 N) (full scale) applied in the $-x$ direction at the top edge of the heat shield would right the overturned vehicle. The heat shield on the model was more dense than water, and when the vehicle was in the upright position, the heat shield extended to form a sea anchor. Waves had little effect on the spacecraft in the upright stable position. It rode well and exhibited no tendency to turn over.

CONCLUDING REMARKS

Landing tests have been made using a 1/4-scale dynamic model of the Apollo command module spacecraft having two different active (deployed-heat-shield) landing-system configurations for impact attenuation. One landing system (configuration 1) consisted of six hydraulic struts and eight crushable honeycomb struts. The other landing system (configuration 2) based on mass estimations was lighter and consisted of four hydraulic struts and six strain straps.

The model investigation indicated that for configuration 1, maximum normal accelerations at the vehicle center of gravity for landings on water and a hard clay-gravel composite landing surface at a simulated vertical velocity of 23 ft/sec (7.0 m/s) were 9g and 18g, respectively. For landings on a sand landing surface at a simulated vertical velocity of 30 ft/sec (9.1 m/s), the maximum normal acceleration was 20g. The maximum normal center-of-gravity acceleration for configuration 2 landing on the hard clay-gravel landing surface at a vertical velocity of 23 ft/sec (7.0 m/s) was approximately 19g.

Accelerations for configuration 2 were generally equal to or lower than accelerations for configuration 1 and normal and longitudinal accelerations for both configurations were considered to be below human acceleration-tolerance limits without using crew-couch shock absorbers or other load-alleviation devices.

Configuration 1 was stable for all landings made on calm water. It was stable on the sand landing surface for landing attitudes from -20° to 5° for a 0° roll landing condition. For landings on a hard clay-gravel composite landing surface, both configurations at 0° roll had a stable region between two unstable regions, the most desirable landing attitude being about -10°. The stability envelopes for configuration 1 were generally slightly larger than those for configuration 2 and stability characteristics for both configurations indicate that roll control of the spacecraft would be desirable.

Configuration 1 was tested for flotation stability and it was found to be stable in an approximately upright attitude. The vehicle in a turned-over condition was righted by waves 2 ft (0.61 m) high and 36 ft (11 m) long.

Langley Research Center,
National Aeronautics and Space Administration,
Langley Station, Hampton, Va., September 29, 1965.

APPENDIX A

CONVERSION OF U.S. CUSTOMARY UNITS TO SI UNITS

The International System of Units (SI) was adopted by the Eleventh General Conference on Weights and Measures, Paris, October 1960, in Resolution No. 12 (ref. 7). Conversion factors for the units used herein are given in the following table:

Physical quantity	U.S. Customary Unit	Conversion factor (*)	SI Unit
Length	in.	0.0254	meters (m)
Area	in^2	6.4516×10^4	$meters^2$ (m^2)
Mass	slug	14.59339	kilograms (kg)
Moment of inertia	$slug\text{-}ft^2$	1.35582	$kilograms\text{-}meters^2$ ($kg\text{-}m^2$)
Velocity	ft/sec	0.3048	meters/second (m/s)
Linear acceleration	ft/sec^2	0.3048	$meters/second^2$ (m/s^2)
Force	lbf	4.448	newtons (N)
Stress	lbf/in^2	6.89×10^3	$newtons/meter^2$ (N/m^2)

*Multiply value given in U.S. Customary Unit by conversion factor to obtain equivalent value in SI Unit.

APPENDIX B

MASS COMPARISON OF LANDING SYSTEMS

Landing system mass estimates for configurations 1 and 2 are shown in the following tables:

	Mass (each)		Total mass	
Configuration 1:				
6 vertical struts (hydraulic)*	0.466 slug	6.80 kg	2.796 slugs	40.80 kg
8 horizontal struts (honeycomb)*	0.310 slug	4.52 kg	2.480 slugs	36.19 kg
Strengthen heat shield to accommodate strut mounting brackets (6 areas)	0.310 slug	4.52 kg	1.860 slugs	27.14 kg
24 mounting brackets on heat shield and at existing hard points on command module structure	0.062 slug	0.90 kg	1.488 slugs	21.71 kg
Total hardware mass			8.624 slugs	125.84 kg
Configuration 2 using nickel strain straps of the material used in the model investigation:				
4 vertical struts (hydraulic)*	0.466 slug	6.80 kg	1.864 slugs	27.20 kg
2 front strain straps	0.610 slug	8.90 kg	1.220 slugs	17.80 kg
2 side strain straps	0.400 slug	5.84 kg	0.800 slug	11.67 kg
2 rear strain straps	0.270 slug	3.94 kg	0.540 slug	7.88 kg
12 fittings on ends of strain straps	0.016 slug	0.23 kg	0.192 slug	2.80 kg
Strengthen heat shield to accommodate strut mounting brackets (5 areas)	0.310 slug	4.52 kg	1.550 slugs	22.62 kg
18 mounting brackets on heat shield and at existing hard points on command module structure	0.062 slug	0.90 kg	1.116 slugs	16.29 kg
Total hardware mass			7.282 slugs	106.26 kg
Configuration 2 using titanium strain straps:				
4 vertical struts (hydraulic)*	0.466 slug	6.80 kg	1.864 slugs	27.20 kg
2 front strain straps	0.097 slug	1.42 kg	0.194 slug	2.83 kg
2 side strain straps	0.066 slug	0.96 kg	0.132 slug	1.93 kg
2 rear strain straps	0.042 slug	0.61 kg	0.084 slug	1.23 kg
12 fittings on ends of strain straps	0.016 slug	0.23 kg	0.192 slug	2.80 kg
Strengthen heat shield to accommodate strut mounting brackets (5 areas)	0.310 slug	4.52 kg	1.550 slugs	22.62 kg
18 mounting brackets on heat shield and at existing hard points on command module structure	0.062 slug	0.90 kg	1.116 slugs	16.29 kg
Total hardware mass			5.132 slugs	74.90 kg

*Mass is based on existing full-scale steel struts.

APPENDIX B

The landing system hardware masses are not optimized and other hardware items may be added to the above lists or masses of listed items may be changed, but the totals for both configurations presented are considered to be comparable. It is assumed that the heat-shield structure will not fail during landing.

REFERENCES

1. Vaughan, Victor L., Jr.: Landing Characteristics and Flotation Properties of a Reentry Capsule. NASA TN D-653, 1961.

2. McGehee, John R.; Hathaway, Melvin E.; and Vaughan, Victor L., Jr.: Water-Landing Characteristics of a Reentry Capsule. NASA MEMO 5-23-59L, 1959.

3. Hoffman, Edward L.; Stubbs, Sandy M.; and McGehee, John R.: Effect of a Load-Alleviating Structure on the Landing Behavior of a Reentry-Capsule Model. NASA TN D-811, 1961.

4. Stubbs, Sandy M.: Landing Characteristics of a Reentry Vehicle With a Passive Landing System for Impact Alleviation. NASA TN D-2035, 1964.

5. Thompson, William C.: Dynamic Model Investigation of the Landing Characteristics of a Manned Spacecraft. NASA TN D-2497, 1965.

6. Bennett, R. V.; and Koerner, F. W.: 1/4 Scale Apollo Impact Attenuation Model. Rept. No. NA62H-513, North Am. Aviation, Inc., Sept. 14, 1962.

7. Mechtly, E. A.: The International System of Units – Physical Constants and Conversion Factors. NASA SP-7012, 1964.

8. Stubbs, Sandy M.: Investigation of the Skid-Rocker Landing Characteristics of Spacecraft Models. NASA TN D-1624, 1963.

9. Webb, Paul, ed.: Bioastronautics Data Book. NASA SP-3006, 1964.

10. Herting, D. N.; Pollock, R. A.; and Pohlen, J. C.: Analysis and Design of the Apollo Landing Impact System. AIAA and NASA Third Manned Space Flight Meeting, CP-10, Am. Inst. Aeron. Astronaut., Nov. 1964, pp. 166-178.

TABLE I.- SCALE RELATIONSHIPS

[λ, scale of model]

Quantity	Full-scale value	Scale factor	Model
Length	l	λ	λl
Area	A	λ^2	$\lambda^2 A$
Mass	M	λ^3	$\lambda^3 M$
Moment of inertia	I	λ^5	$\lambda^5 I$
Time	t	$\sqrt{\lambda}$	$\sqrt{\lambda}\, t$
Velocity	v	$\sqrt{\lambda}$	$\sqrt{\lambda}\, v$
Linear acceleration	a	1	a
Angular acceleration	α	λ^{-1}	$\lambda^{-1}\alpha$
Force	F	λ^3	$\lambda^3 F$

TABLE II.- PERTINENT PARAMETERS OF SPACECRAFT

	1/4-scale model		Full-scale vehicle	
Configuration 1:				
Mass	3.56 slugs	51.95 kg	223.6 slugs	3263 kg
Moment of inertia (heat shield retracted) –				
I_X (roll)	3.82 slug ft^2	5.18 kg m^2	3910 slug ft^2	5301 kg m^2
I_Y (pitch)	3.37 slug ft^2	4.57 kg m^2	3450 slug ft^2	4678 kg m^2
I_Z (yaw)	2.09 slug ft^2	2.83 kg m^2	2140 slug ft^2	2901 kg m^2
Body –				
Diameter	37.88 in.	0.962 m	151.52 in.	3.85 m
Height (heat shield retracted)	20.93 in.	0.532 m	83.72 in.	2.13 m
Configuration 2:				
Mass	4.36 slugs	63.6 kg	279.5 slugs	4079 kg
Moment of inertia (heat shield retracted) –				
I_X (roll)	4.19 slug ft^2	5.68 kg m^2	4290 slug ft^2	5816 kg m^2
I_Y (pitch)	3.48 slug ft^2	4.72 kg m^2	3560 slug ft^2	4827 kg m^2
I_Z (yaw)	2.91 slug ft^2	3.95 kg m^2	2980 slug ft^2	4040 kg m^2
Body –				
Diameter	37.88 in.	0.962 m	151.52 in.	3.85 m
Height (heat shield retracted)	20.93 in.	0.532 m	83.72 in.	2.13 m

TABLE III.- INSTRUMENTATION CHARACTERISTICS

Accelerometer orientation	Range, g units	Natural frequency, cps (Hz)	Damping, percent of critical damping	Limiting flat frequency of other recording equipment, cps (Hz)
Configuration 1				
Water landing surface:				
Normal (at vehicle center of gravity)	±100	725	61	190
Longitudinal (at vehicle center of gravity) . .	±50	624	70	190
Angular (pitch)	±200	900	60	190
Normal (at couch center of gravity)	±50	465	89	190
Sand landing surface:				
Normal (at vehicle center of gravity)	±100	725	61	190
Longitudinal (at vehicle center of gravity) . .	±50	624	70	190
Transverse (at vehicle center of gravity) . .	±25	360	59	135
Angular (pitch)	±50	315	55	190
	±100	675	60	190
	±200	900	60	190
Normal (at couch center of gravity)	±50	465	89	190
Longitudinal (at couch center of gravity) . . .	±25	465	52	135
Hard clay-gravel composite landing surface:				
Normal (at vehicle center of gravity)	±100	725	61	240
Longitudinal (at vehicle center of gravity) . .	±50	624	70	240
Angular (pitch)	±200	900	60	240
Normal (at couch center of gravity)	±50	465	89	240
Configuration 2				
Hard clay-gravel composite landing surface:				
Normal (at vehicle center of gravity)	±100	725	61	240
Longitudinal (at vehicle center of gravity) . .	±50	624	70	240
Transverse (at vehicle center of gravity) . .	±25	360	59	120
Angular (pitch)	±200	900	60	120
Normal (at couch center of gravity)	±50	610	55	240
Longitudinal (at couch center of gravity) . . .	±25	355	60	120

TABLE IV.- MAXIMUM ACCELERATION DATA FOR CONFIGURATION 1

[All values are full scale]

(a) Water landing surface

Vertical velocity		Horizontal velocity		Attitude			Normal acceleration at center of gravity, g units	Longitudinal acceleration at center of gravity, g units	Angular acceleration, rad/sec^2	Normal acceleration at couch, g-units
ft/sec	m/s	ft/sec	m/s	Pitch, deg	Roll, deg	Yaw, deg				
23	7.0	0	0	1	0	0	6.6	-2.9	-20 7	8.6
↓	↓	↓	↓	-5	↓	↓	7.4	2.8 -3.0	21 -34	9.6
		10	3.0	-5			5.8	3.5 -2.8	36	6.9
		20	6.1	-1			7.6	3.0 -1.5	21	8.6
		30	9.1	0			7.4	3.7	14 -14	8.6
		↓	↓	-9			5.6	6.5 -4.9	40	6.2
				-14			5.4	4.7	40 -27	7.2
				-19			3.7	4.8	68	4.7
				2			7.2	2.0	0	6.3
				6			7.4	-2.4 3.5	21 -14	7.1
				11			8.3	-4.6 5.6	-41 48	9.9
				15			9.1	-7.1 6.2	-48 21	8.6
		↓	↓	20	↓	↓	7.4	-8.4 6.8	-41 34	8.9
		40	12.0	1	0	0	8.2	4.7	-20 34	9.4
		50	15.0	-2	↓	↓	8.6	-3.5 8.1	56 -28	10.1
		30	9.1	6	180	0	8.5	-3.0	14 -55	11.9
↓	↓	50	15.0	8	↓	↓	8.3	-3.5	21 -55	12.7
30	9.1	30	9.1	8	↓	↓	12.2	-8.1	54 -68	16.7
↓	↓	↓	↓	1	0	0	12.7	'6.3	-41 48	15.7
↓	↓	0	0	2	↓	↓	10.6	-5.2 4.7	40 -27	12.8

TABLE IV.- MAXIMUM ACCELERATION DATA FOR CONFIGURATION 1 – Continued

(b) Sand landing surface

Vertical velocity		Horizontal velocity		Attitude			Normal acceleration at center of gravity, g units	Longitudinal acceleration at center of gravity, g units	Angular acceleration, rad/sec^2	Normal acceleration at couch, g units	Longitudinal acceleration at couch, g units	Transverse acceleration at center of gravity, g units	Remarks
ft/sec	m/s	ft/sec	m/s	Pitch, deg	Roll, deg	Yaw, deg							
30	9.1	0	0	0	0	0	19.8	-7.9	-25 30	21.6	-6.4		
↓	↓	↓	↓	↓	↓	↓	16.7	-5.1	-15 15	17.0	-4.3		
							18.2	-6.7	-25 36	20.4	-6.0		
							18.1	-5.2	-26 26	23.7	-4.0		
				-5			15.8	8.5	59	17.5	8.9		
				-7			17.2	11.4	79	16.0	8.9		
				-15			15.2	15.8	122	11.9	15.8		
		↓	↓	-15			11.8	14.2	102	14.3	14.7		
		15	4.6	-1			18.1	7.8	-55	19.4	8.9		
		↓	↓	-5			15.9	11.8	64 -59	18.4	12.9		
				-10			13.6	16.4	96 -46	17.9	16.3		
				-15			13.8	18.7	95 -13	14.6	16.9		
				-20			11.6	16.4	95	13.6	16.7		
				5			15.9	6.6	-100	18.4	6.0		
				10			13.6	-4.7 7.6	-95	20.6	-4.2 6.5		
				15			12.7	-8.0 2.6	-86	21.3	-7.1		
		↓	↓	20			10.9	-8.5	-95	21.1	-9.4		
		30	9.1	-2			18.1	15.8	36 -88	23.5	17.2		
		↓	↓	-4			16.3	18.0	39 -79	23.3	15.2		
				-9			15.4	17.0	79 -33	18.4	16.1		
				-13			11.8	18.0	117 -51	15.8	18.5		
				3			15.4	14.2	-108	24.2	14.0		
				6			13.1	14.2	-91	20.9	13.4		
				7			13.6	16.1	-112	23.5	14.7		
		↓	↓	17			13.6	13.7 -5.0	-153	30.1	14.5 -5.8		Turned over
		40	12.0	0			14.9	16.1	-119	23.3	16.1		
		↓	↓	-2			15.9	14.7	37 -78	20.4	14.0		
				-2			15.9	14.2	37 -87	20.4	14.9		
				-9			13.6	15.6	100 -28	15.8	15.6		
				-14			12.7	15.6	115	13.3	16.1		
				-20			13.1	14.2	128	10.2	13.8		
				1			16.3	16.8	-125	25.2	17.2		
				5			14.9	15.6	-104	22.3	16.1		
				10			15.5	16.0	-194	31.8	17.8		
		↓	↓	15			16.8	18.2	-200	34.9	16.1		Turned over
		50	15.0	-2			15.4	15.1	36 -71	23.7	14.3		
		↓	↓	-8			15.0	18.9	102	17.0	14.5		
				-10			14.5	15.1	92	15.0	14.3		
				2			17.2	15.1	-102	23.0	16.7		
				3			14.5	16.1	-127	25.0	16.7		
				7			16.8	16.6	-127	28.9	15.2		
		↓	↓	13	↓	↓	15.8	16.6	-153	29.3	15.2		Turned over
		15	4.6	-5	90	0	17.2	4.7	50	15.5	4.9	8.2	
		30	9.1	-5	↓	↓	17.2	4.7	62	16.0	4.2	14.9	
		40	12.0	-5			14.5	3.3	44	15.3	2.9	16.1	
		50	15.0	-5			18.1	3.5	31	18.0	4.9	13.5	
		↓	↓	-10	↓	↓	18.1	5.7	44	18.7	4.9	12.2	
				-10	180	0	18.6	-11.3	124	17.2	-12.5		
↓	↓	↓	↓	-15	↓	↓	16.8	-9.2	112	18.0	-10.7		

TABLE IV.- MAXIMUM ACCELERATION DATA FOR CONFIGURATION 1 – Continued

(c) Hard clay-gravel landing surface

Vertical velocity		Horizontal velocity		Attitude			Normal acceleration at center of gravity, g units	Longitudinal acceleration at center of gravity, g units	Angular acceleration, rad/sec^2		Normal acceleration at couch, g units		Remarks
ft/sec	m/s	ft/sec	m/s	Pitch, deg	Roll, deg	Yaw, deg							
23	7.0	0	0	0	0	0	16.6	-7.3	-30	36	18.4		
↓	↓	↓	↓	1	↓	↓	17.3	-6.9	-30	54	20.5		
				0			18.0	-3.5	-36		21.3		
				-5			16.3	8.3	85	-67	18.4		
				-10			13.4	14.1	114	-54	16.7		
				-15			11.2	15.5	114		11.3		
				-20			10.4	14.1	102		-3.3	9.6	
				-25			10.4	15.9	114		-7.5	9.2	
		↓	↓	-30			8.8	14.8	114		-12.0	9.6	
		10	3.0	0			17.6	7.6	-91		23.4		
		↓	↓	-5			15.9	15.9	49	-121	26.4		
				-15			11.1	15.5	103		14.2		
				-20			12.1	15.5	84		-1.7	11.3	
				-25			10.1	15.9	108		-6.7	10.9	
		↓	↓	-30			8.6	15.2	103		-5.8	84.0	
		20	6.1	1			18.3	15.5	-175		32.2		
		↓	↓	-3			16.4	16.9	-119		28.0		
				-10			14.6	17.9	108	-66	18.8		
				-14			13.0	17.3	96		14.2		
				-20			10.4	13.3	89		-4.6	8.4	
		↓	↓	-25			9.5	15.9	138		-11.7	8.4	
		30	9.1	1			16.4	17.6	-154		28.9		
		↓	↓	-4			15.6	12.9	42	-84	21.8		
				-10			12.7	13.8	90	-60	18.0		
				-15			11.4	13.9	90		12.6		
				-20			10.1	13.1	108		-5.4	8.4	
				-25			9.5*	14.5*	132		-7.1	8.0*	Turned over
		↓	↓	-30			8.5*	13.1*	114		-8.4	7.5*	Turned over
		40	12.0	0			13.4	9.0	-95		21.3		
↓	↓	↓	↓	-3	↓	↓	14.3	11.0	-125		21.3		

*Maximum accelerations were higher during turnover.

TABLE IV.- MAXIMUM ACCELERATION DATA FOR CONFIGURATION 1 – Concluded

(c) Hard clay-gravel landing surface – Concluded

Vertical velocity		Horizontal velocity		Attitude			Normal acceleration at center of gravity, g units	Longitudinal acceleration at center of gravity, g units	Angular acceleration, rad/sec^2	Normal acceleration at couch, g units	Remarks
ft/sec	m/s	ft/sec	m/s	Pitch, deg	Roll, deg	Yaw, deg					
23	7.0	40	12.0	-10	0	0	12.6	14.7	66 -60	18.4	
↓	↓	↓	↓	-14	↓	↓	12.0	14.8	84	13.0	
				-20			11.3	14.1	71	-4.2 8.4	
				-25			9.8*	12.4*	110*	-10.0 6.7*	Turned over
		↓	↓	-30			8.3*	13.5*	114*	-10.0 7.5*	Turned over
		50	15.0	5			13.7	13.5	-102	20.1	Turned over
		↓	↓	-1			16.3	14.8	-125	25.1	
				-9			15.0	14.5	71 -53	19.7	
				-14			11.7	14.4	102	13.4	
				-20			10.0	13.0	109	-6.3 9.2	
		↓	↓	-24	↓		10.0	11.9	134	-12.0 6.7	
		30	9.1	0	90		16.3	-4.6	30	18.8	
		↓	↓	-2	↓		15.3	2.8	24	16.7	
				-8			14.3	7.2	84	15.5	
				-9			15.0	8.8	97 -36	15.5	
				-9			15.0	8.4	91	16.3	
				-13			11.6	13.0	91	11.3	
				-16	↓		10.3	13.0	86	8.0	
				-1	180		18.6	-16.4	97	13.8	
				-6	↓		14.0	-14.0	104	13.8	
				-10			13.0	-14.0	109	10.5	
				-16			10.8*	-13.3	104	13.8*	Turned over
				-22			10.8*	8.8 -13.6*	110	14.7*	Turned over
				-26			14.7*	12.6 -11.6*	98 -73*	20.9*	Turned over
		↓	↓	-30	↓		15.6*	12.2 -11.6*	122 -73*	23.9*	Turned over
		0	0	-30	0		10.1	21.0	114	10.9	
		10	3.0	-30	↓		10.0	15.5	115	8.8	
		5.0	1.5	-30	180		9.6	12.1	140	9.2	
		7.5	2.3	-30	↓		8.2*	10.3*	150	-10.5 5.9	Turned over
↓	↓	10.0	3.0	-30	↓	↓	8.3*	10.5*	127	6.3*	Turned over

*Maximum accelerations were higher during turnover.

TABLE V.- MAXIMUM ACCELERATION DATA FOR CONFIGURATION 2 ON HARD CLAY-GRAVEL LANDING SURFACE

[All values are full scale; L denotes left, R denotes right]

Vertical velocity		Horizontal velocity		Attitude			Normal acceleration at center of gravity, g units	Longitudinal acceleration at center of gravity, g units	Angular acceleration, rad/sec^2		Normal acceleration at couch, g units	Longitudinal acceleration at couch, g units	Transverse acceleration at center of gravity, g units	Remarks
ft/sec	m/s	ft/sec	m/s	Pitch, deg	Roll, deg	Yaw, deg								
23	7.0	0	0	-4	0	0	18.3	7.1	-71	39	18.7	7.1	3.3	
↓	↓	↓	↓	-4	↓	↓	18.4	6.6	-71	55	18.7	6.7	1.8	
				-5			17.4	8.0	-68	55	18.1	6.7	2.2	
				-9			16.2	8.6	65	-63	15.5	9.3	2.4	
				-14			13.3	10.2	79	-31	12.6	10.0	2.2	
				-19			9.5	10.7	74		10.2	10.2	1.3	
				-25			7.2	10.2	60		7.6	8.4	2.0	
				-29			7.9	8.5	52		7.4	8.8	1.5	
				5			15.5	-5.6	-103	60	19.4	-7.0	1.3	
		↓	↓	10			12.7	-6.8	-131	26	18.9	-7.0	2.4	
		10	3.0	-1			17.4	7.8	-99		18.3	7.5	3.9	
				-4			17.8	8.8	-86	26	19.2	9.0	3.3	
				-10			16.3	9.6	-57	47	17.4	10.2	3.2	
				-15			14.9	8.7	66		14.6	10.3	1.5	
				-20			10.1	9.6	60		11.3	9.9	1.7	
				-24			7.2	10.0	50		8.3	8.5	1.9	
				-29			7.7	8.8	58		9.3	8.7	1.9	
				5			17.1	6.2	-103		17.9	6.4	1.5	
		↓	↓	10			12.9	-1.7 2.8*	-130		18.3	-2.5 2.6*	1.9*	Turned over
		20	6.1	-2			18.6	9.3	-92		20.5	9.8	3.1	
				-7			17.1	8.6	39	-52	20.2	9.2	3.3	
				-11			15.2	9.2	60		16.6	10.2	2.2	
				-17			11.0	8.9	52		11.5	9.1	3.2	
				-22			7.9	9.4	57		8.7	7.0	1.7	
				-28			7.2	7.4	60	-52	10.4	7.1	3.0	
				1			17.9	9.4	-105	53	21.5	9.1	1.3	
		↓	↓	5			16.2*	10.0*	-95	53	19.2*	9.6*	1.1*	Turned over
				10			14.7*	8.6*	-132	50*	20.9*	8.4*	1.1*	Turned over
		30	9.1	-1			17.6	9.2*	-86		18.3	8.1*	3.2	Turned over
				-5			17.4	9.2	-84		17.6	8.9	3.3	
				-7			16.6	7.8	23	-73	17.0	8.2	3.5	
				-11			13.0	7.2	55	-34	13.0	7.7	3.0	
				-20			10.6	7.6	55		10.2	7.2	1.9	
				-22			7.6*	9.4*	52	-50*	9.3*	7.9*	2.4*	Turned over
				-27			7.9*	8.2*	52	-39*	10.7*	8.3*	1.9*	Turned over
				6			14.5*	7.8*	-106*		17.9*	6.5*	2.6*	Turned over
↓	↓	↓	↓	10	↓	↓	15.2*	8.6*	-106	44*	17.4*	7.1*	1.3*	Turned over

*Maximum accelerations were higher during turnover.

TABLE V.- MAXIMUM ACCELERATION DATA FOR CONFIGURATION 2 ON HARD CLAY-GRAVEL LANDING SURFACE – *Concluded*

Vertical velocity		Horizontal velocity		Attitude			Normal acceleration at center of gravity, g units	Longitudinal acceleration at center of gravity, g units	Angular acceleration, rad/sec^2	Normal acceleration at couch, g units	Longitudinal acceleration at couch, g units	Transverse acceleration at center of gravity, g units	Remarks
ft/sec	m/s	ft/sec	m/s	Pitch, deg	Roll, deg	Yaw, deg							
23	7.0	40	12	0	0	0	17.4*	9.3*	-94 26*	20.0*	8.8*	1.3*	Turned over
↓	↓	↓	↓	-4	↓	↓	27.6	9.3	-60 29	29.0	10.4	2.4	Heat shield bottomed
				-9			16.0	9.8	52 -50	16.1	10.6	1.6	
				-14			14.1	7.9	60 -18	13.7	9.0	2.8	
				-20			10.5*	8.3*	52 -31*	9.6*	9.4*	1.5*	Turned over
				-25			7.4*	7.7*	50 -35*	9.6*	7.8*	2.6*	Turned over
				-30			7.2*	8.2*	47 -39*	11.5*	7.8*	1.9*	Turned over
				4			16.3*	8.1*	-99 16*	18.3*	7.2*	2.4*	Turned over
		↓	↓	9			13.8*	7.6*	-117 44*	17.6*	6.7*	1.5*	Turned over
		50	15	-3			19.0	9.6	-83 26	21.6	8.5	1.5	
				-3			19.3	8.5	-80 31	18.0	8.8	3.2	
				-10			15.2	8.1	57 -60	17.0	8.2	3.5	
				-15			12.8	8.4	60 -39	14.0	9.5	2.6	
				-20			10.3*	8.6*	63 -13*	10.0*	8.3*	2.4*	Turned over
				-25			9.0*	9.2*	56 -40*	9.8*	8.8*	1.3*	Turned over
				-30			7.8*	8.8*	59 -39*	11.8*	9.3*	1.1*	Turned over
		↓	↓	5	↓		16.3*	8.9*	-130 29*	19.6*	7.4*	.6*	Turned over
		30	9.1	0	90L		18.6	-2.6 3.0	-49 31	17.6	2.1 -3.8	-9.2	
				-3			19.9	8.0	47 -42	19.6	4.0	-9.4	
				-9			13.3	5.3	70 -31	16.1	7.2	-7.4	
				-13			15.4	4.9	80 -23	16.8	5.1	-7.6	
				-18			13.0	7.8	85 -21	8.7	8.5	-8.0	
				-24			8.8	7.5	101	-3.1 8.7	6.0 -1.5	-7.5 1.3	
				-27			7.8	7.6	69 -44	-5.6 11.5	5.7 -1.4	-7.1	
				3			17.9	-3.5 4.2	-60 23	16.8	-3.5 2.9	-8.6	
		↓	↓	8			15.5	-2.8	-93 20	17.9	-4.2	-9.0	
		50	15.0	-1			16.4*	5.4 -2.8*	-46 38*	15.6*	-4.8 3.3*	-11.3*	Turned over
				-10			13.8*	9.4 -4.2*	72 -33*	16.3*	7.1 -2.4*	-11.5*	Turned over
				-20			9.5*	6.6*	80*	11.3*	6.7 -1.3*	-10.2*	Turned over
		↓	↓	10	↓	↓	12.1*	-4.2*	-106*	15.4*	-4.8*	5.5*	Turned over
		30	9.1	-10	90L	14L	18.3*	3.5*	57*	15.2*	3.8*	-7.1*	Turned over
		↓	↓	-9	90R	13L	18.8	4.0 -1.6*	57	16.8	3.6	10.0	Turned over
		↓	↓	-8	0	9L	14.3	8.5	41 -47	15.5	7.0	6.9	
		10	3.0	-18	180	0	12.1	6.4	108 -26	13.4	5.7 -1.4	2.0 -2.2	
		↓	↓	-25	↓	↓	8.3*	6.7*	103 -36	10.7	6.3 -2.6	1.5	Turned over
		30	9.1	-5			16.4	-8.8	79 -48	17.2	-7.8	2.6 -3.2	
				-10			16.4*	-10.8*	81 -39*	16.5*	-10.0*	2.7 -3.1*	Turned over
				-15			15.6	-13.9	138 -34	17.2	-14.4	1.7	
				2			17.0	-5.9	44 -56	18.9	-6.0	2.1 -3.3	
				3			16.4	-7.2	59 -54	18.7	-7.2	1.1 -2.9	
		↓	↓	9			13.7	-6.6	-95 44	15.5	-7.0	1.0 -1.3	
		50	15.0	-1			15.7	-8.5	72 -118	13.8	5.3 -6.7	1.7 -2.0	
				-7			19.5	-9.2	95 -31	18.2	2.1 -7.9	2.5 -4.0	
				-11			16.4*	-9.6*	110 -23*	14.7*	2.8 -10.4*	7.8 -7.1	Turned over
↓	↓	↓	↓	5	↓	↓	17.3	-6.8	-77 54	16.3	-6.7	2.8 -2.4	

*Maximum accelerations were higher during turnover.

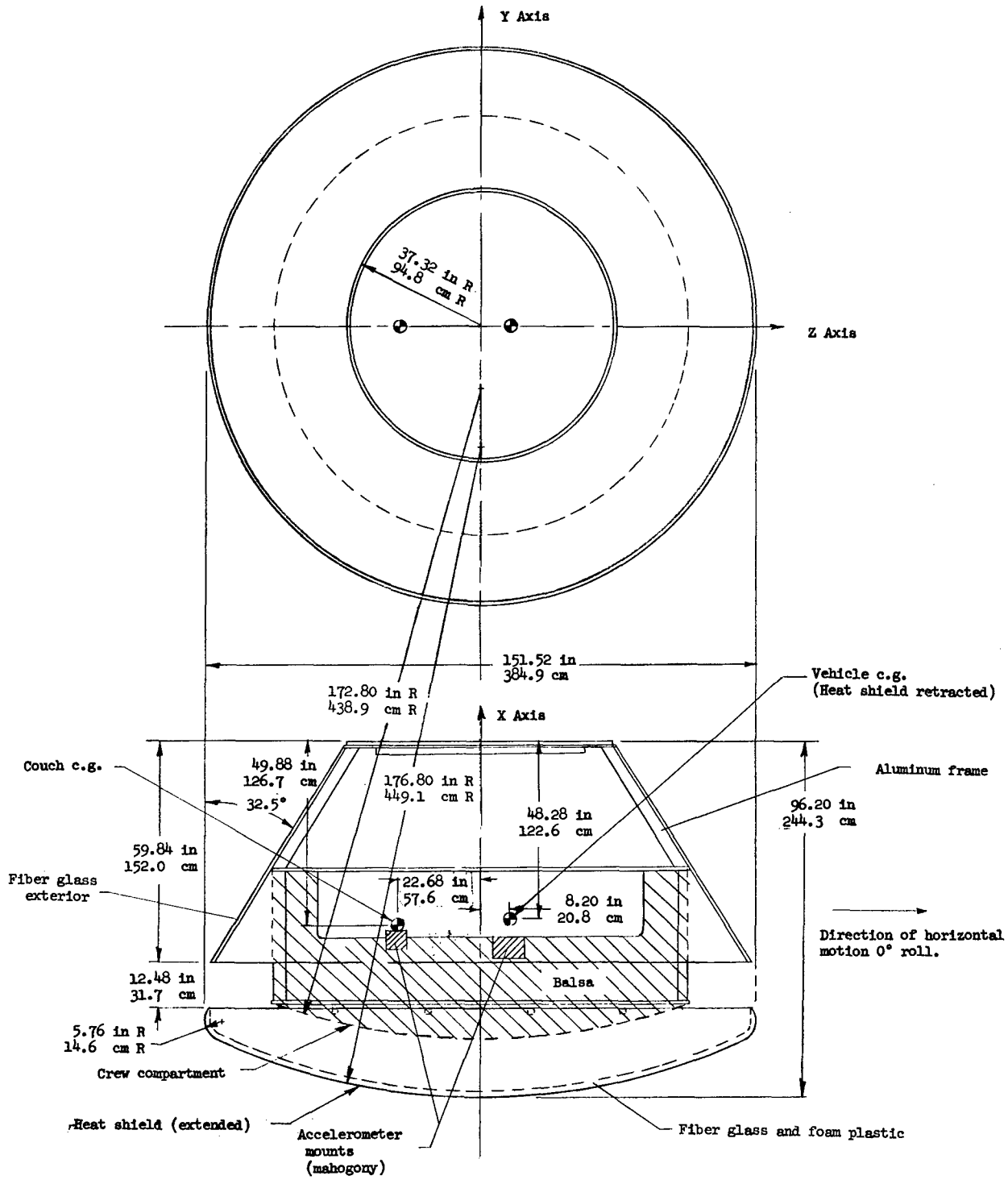

Figure 1.- General arrangement of 1/4-scale dynamic model of configuration 1. All values are full scale.

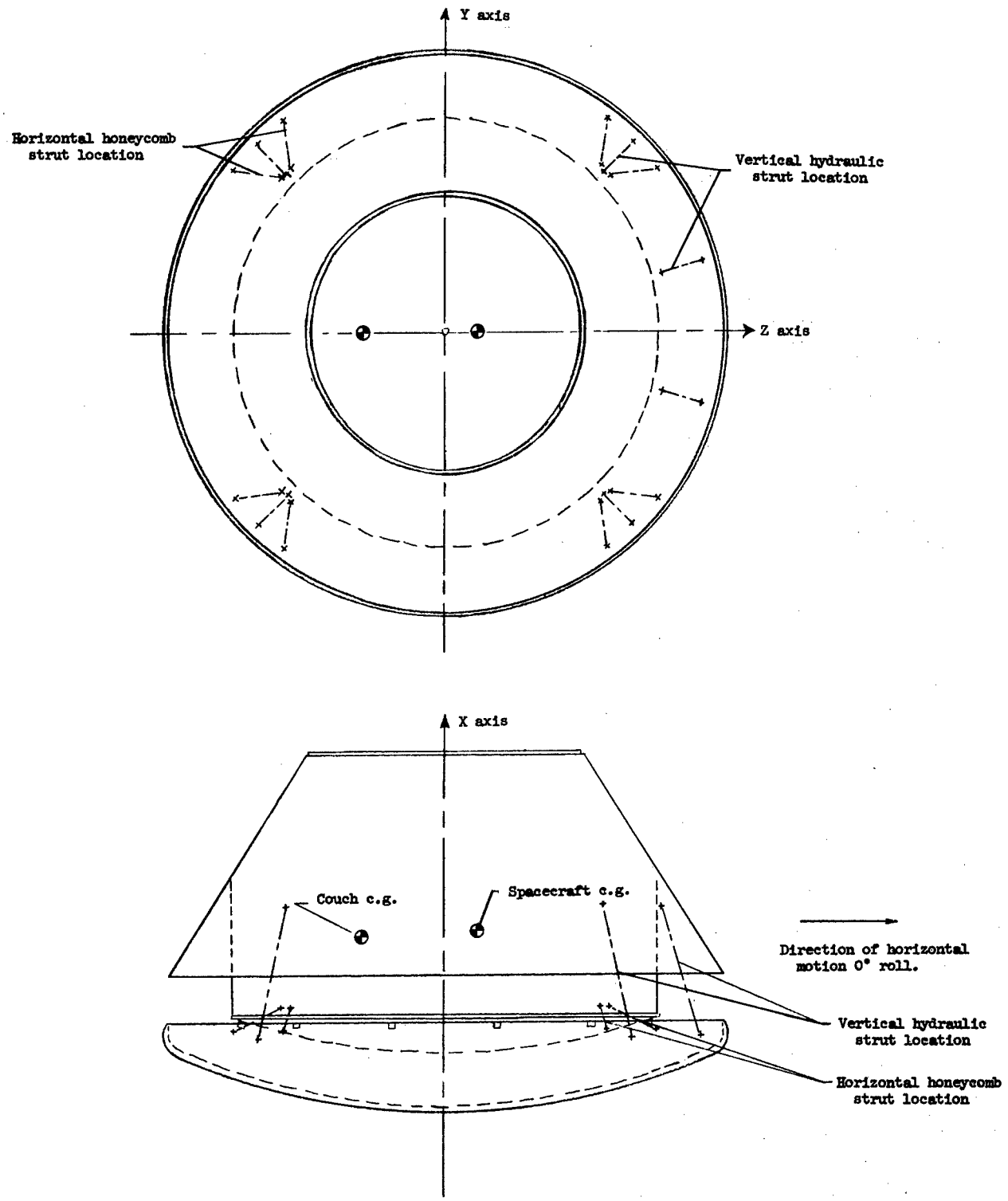

Figure 2.- Location of landing-gear components for configuration 1.

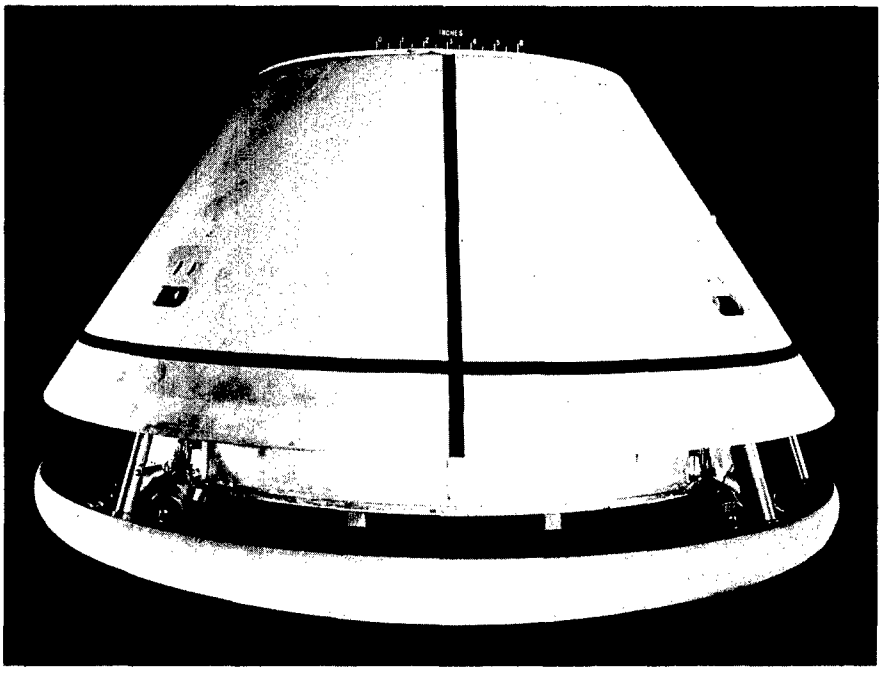

Side view L-62-6680

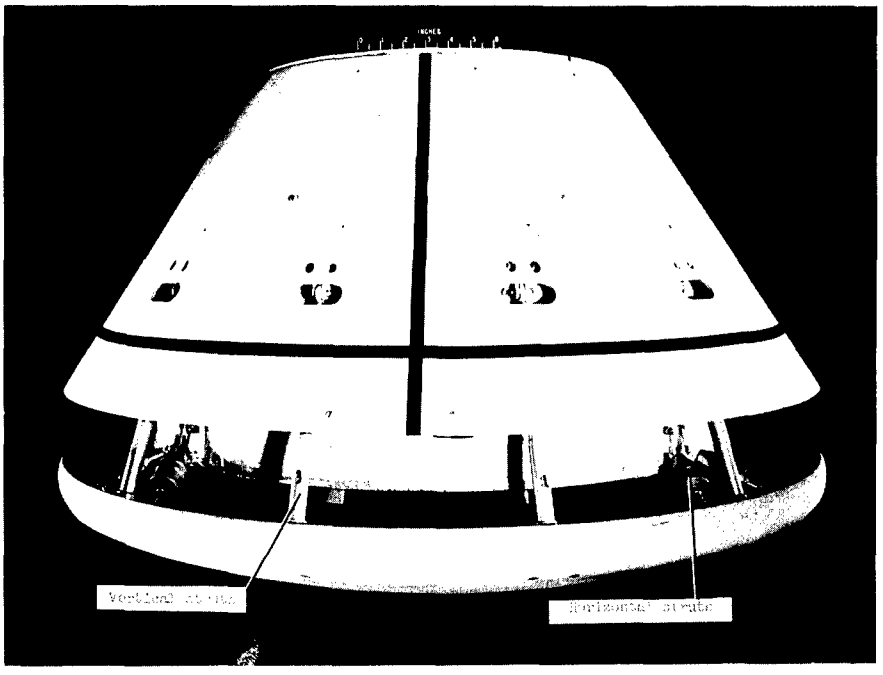

Front view L-62-6679

Figure 3.- Photograph of configuration 1.

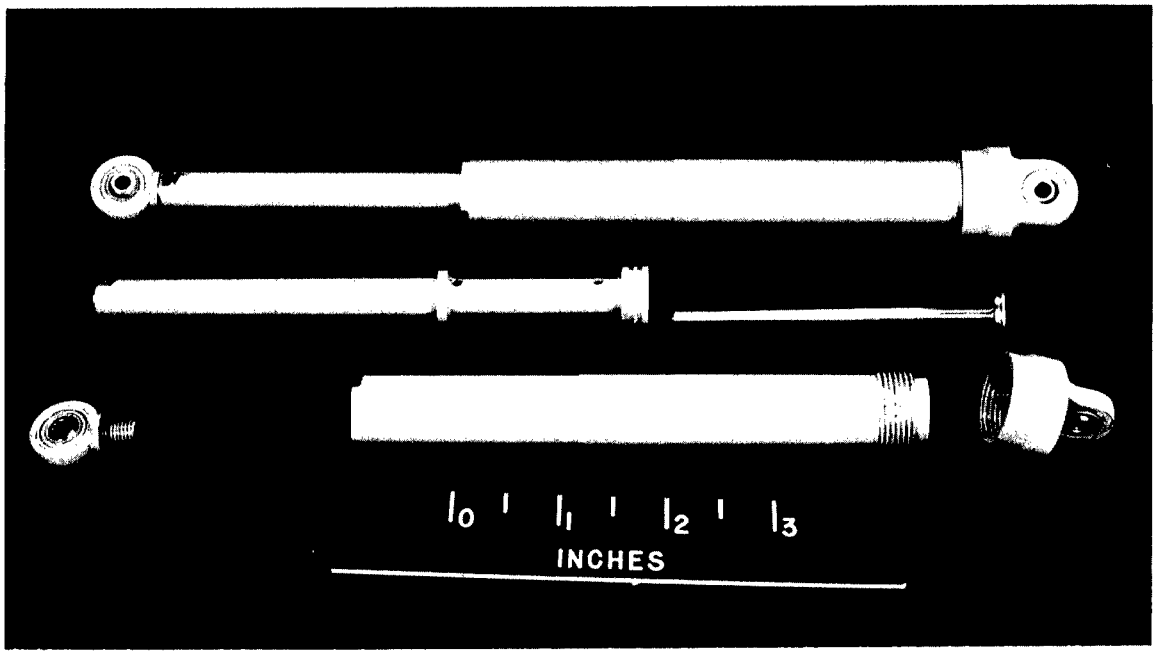

(a) Vertical strut (hydraulic) of configurations 1 and 2. L-63-6189

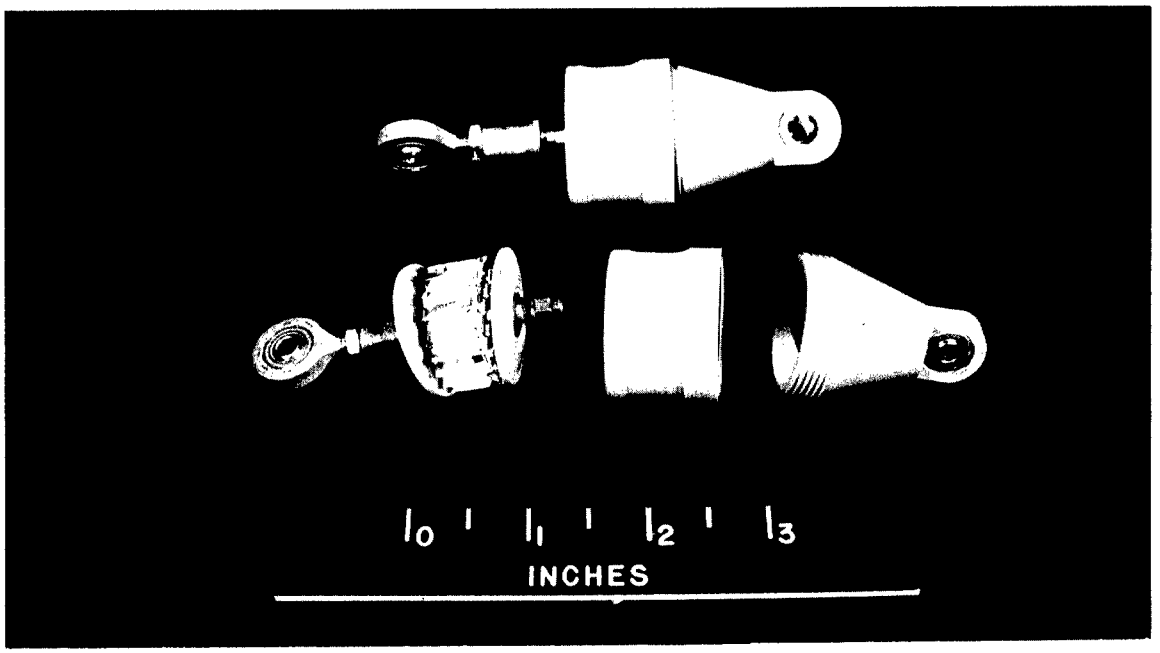

(b) Horizontal struts of configuration 1. L-63-6188

Figure 4.- Landing system elements.

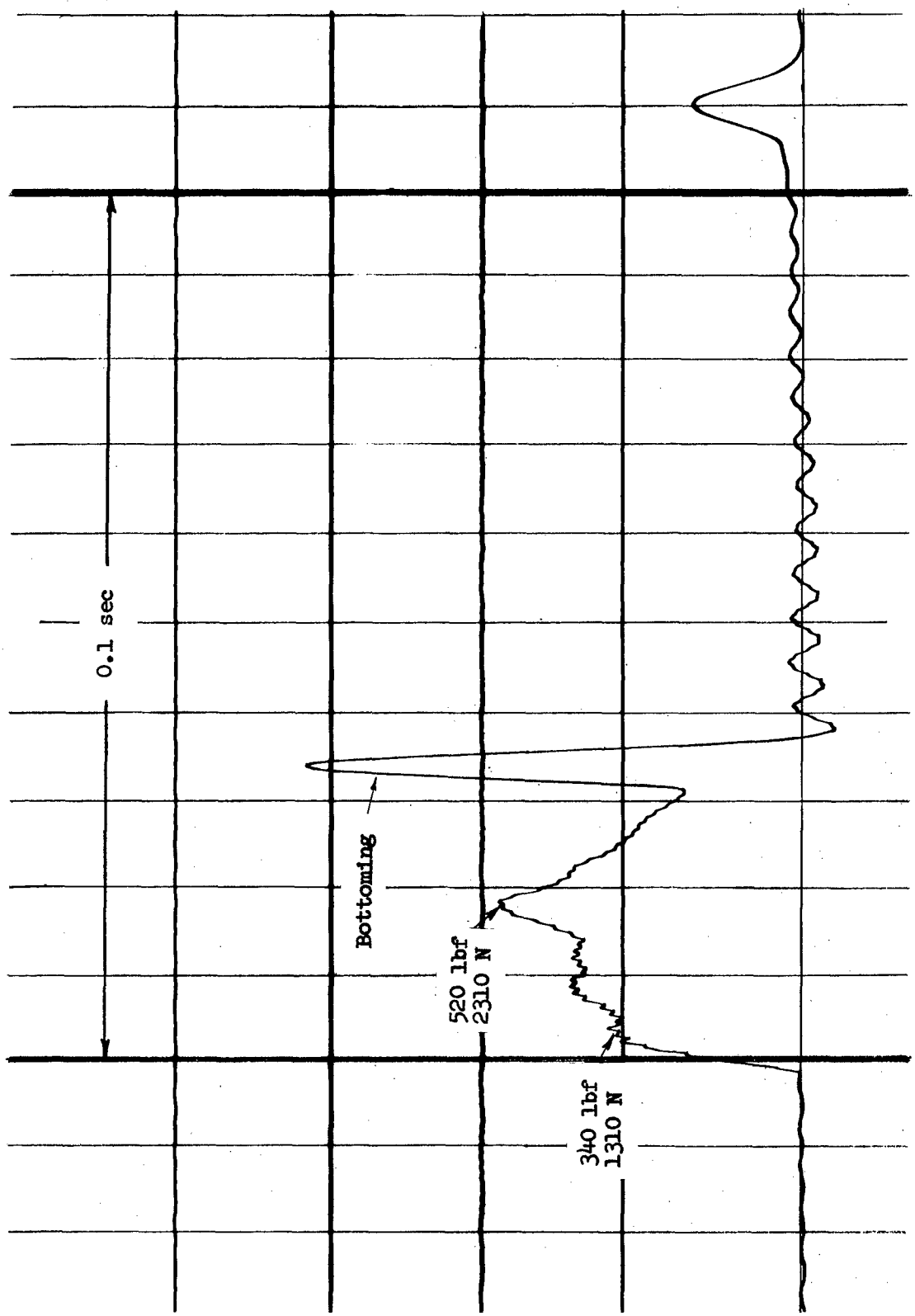

Figure 5.- Force characteristics for vertical hydraulic shock strut used with configuration 1. All values are model scale. Impacting mass, 0.89 slug (12.98 kg); velocity at impact, 15 ft/sec (4.6 m/s).

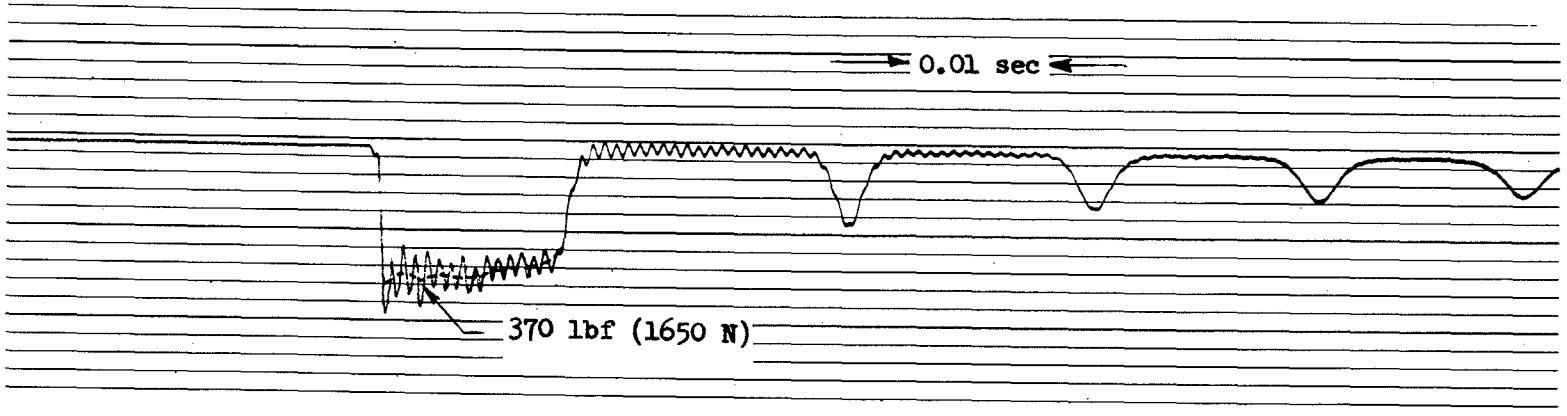

Figure 6.- Force characteristics for honeycomb used in horizontal shock struts on configuration 1. Values are model scale. Honeycomb wall thickness 0.002 in. (0.051 mm); impacting mass, 0.85 slug (12.4 kg); velocity at impact, 4.4 ft/sec (1.3 m/s).

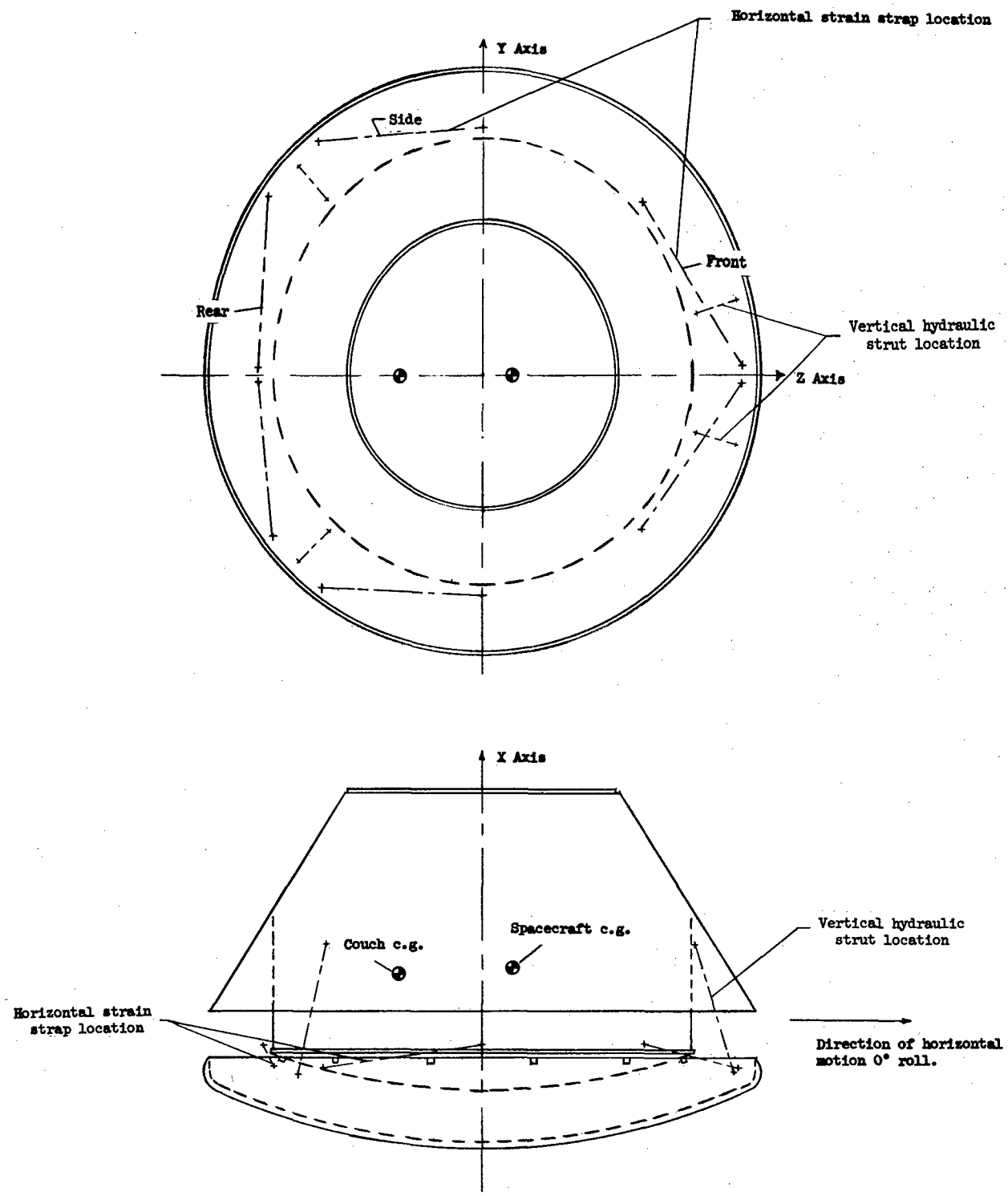

Figure 7.- Location of landing-gear components for configuration 2.

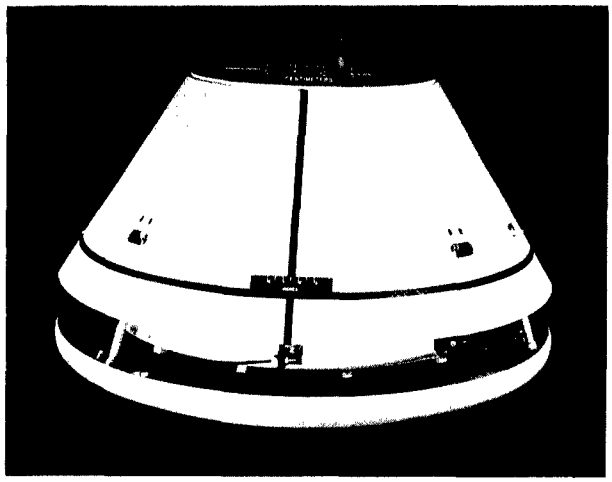

Side view L-64-5269

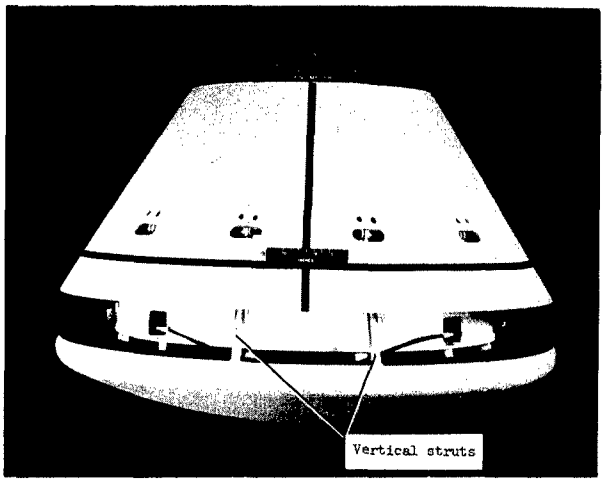

Front view L-64-5270

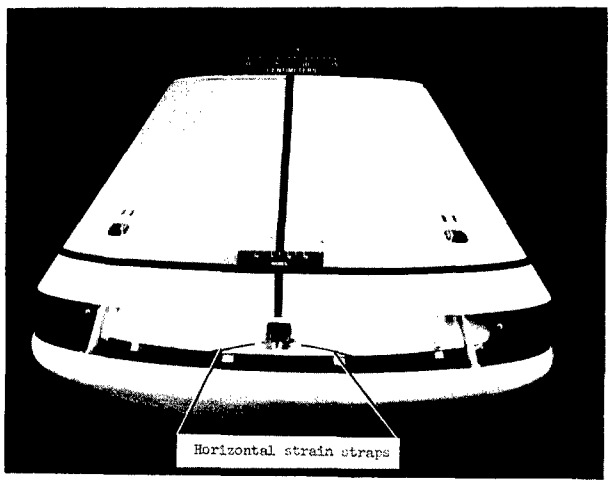

Rear view L-64-5273

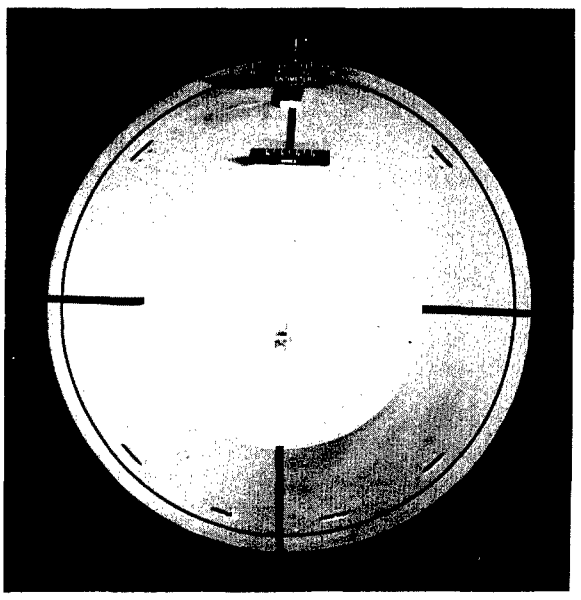

Top view L-64-5272

Figure 8.- Photographs of configuration 2.

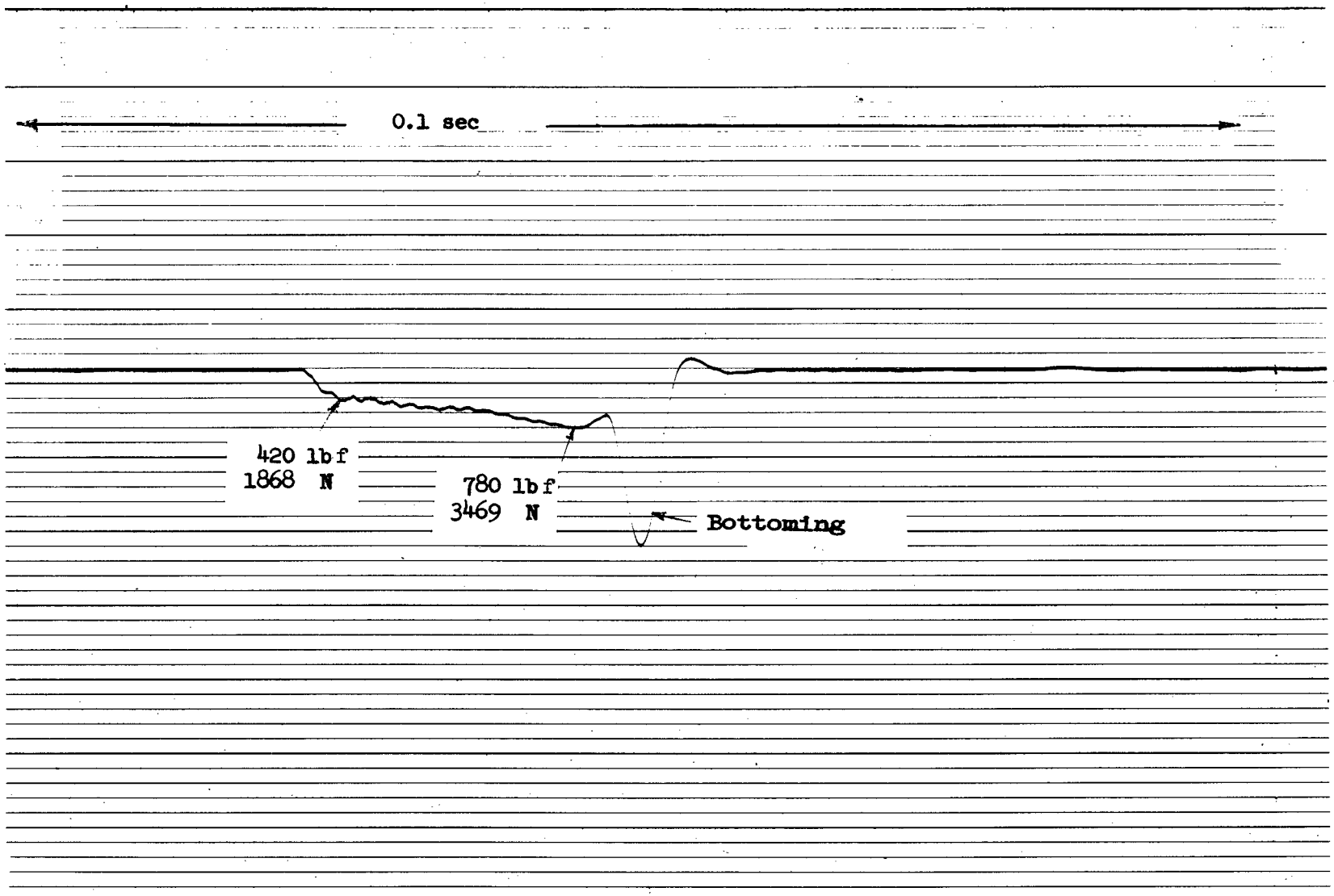

Figure 9.- Force characteristics for vertical hydraulic strut used with configuration 2. All values are model scale. Impacting mass, 1.24 slugs (18.1 kg); velocity at impact, 15 ft/sec (4.6 m/s).

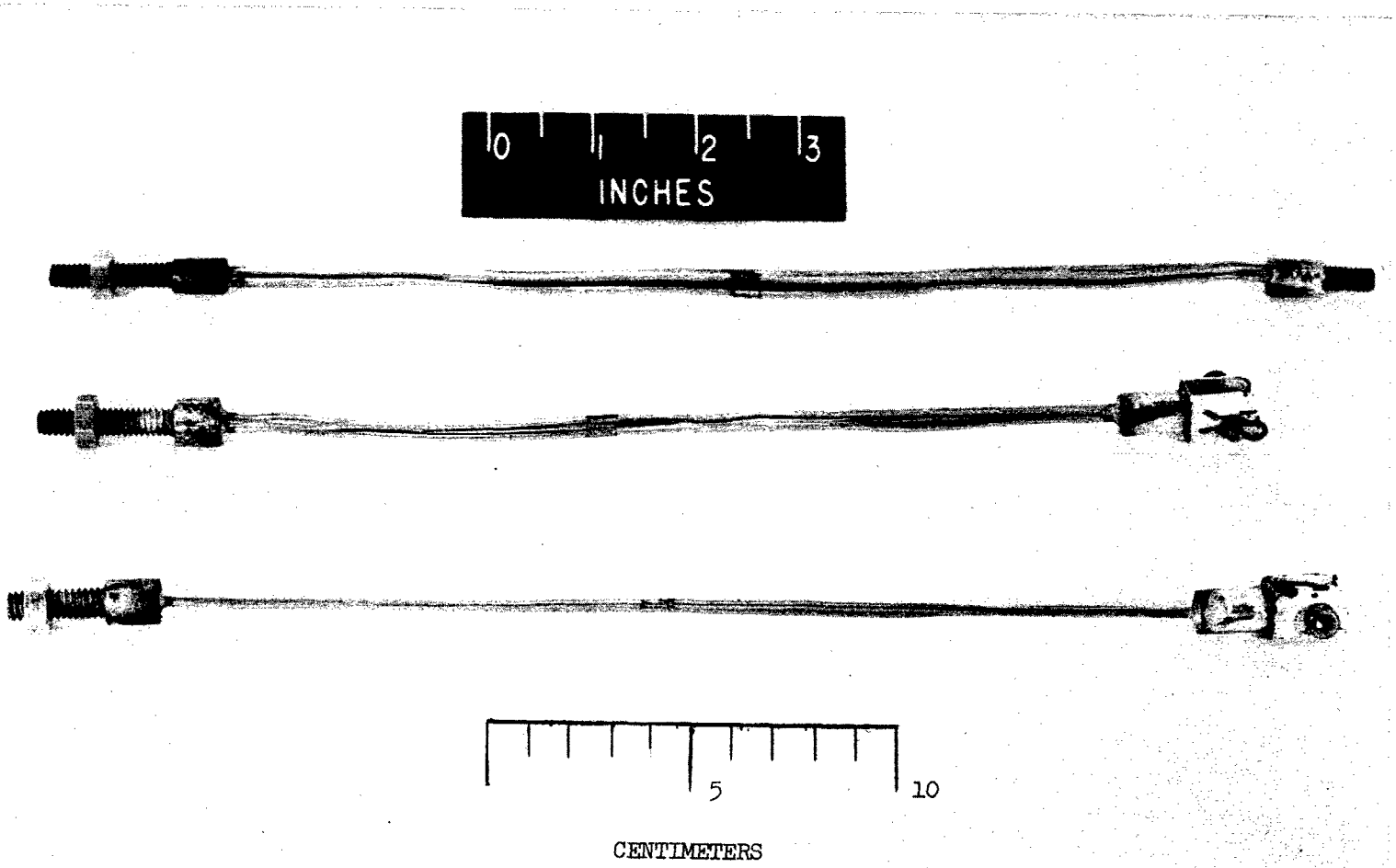

Figure 10.- Horizontal strain straps used on configuration 2.

L-65-7912

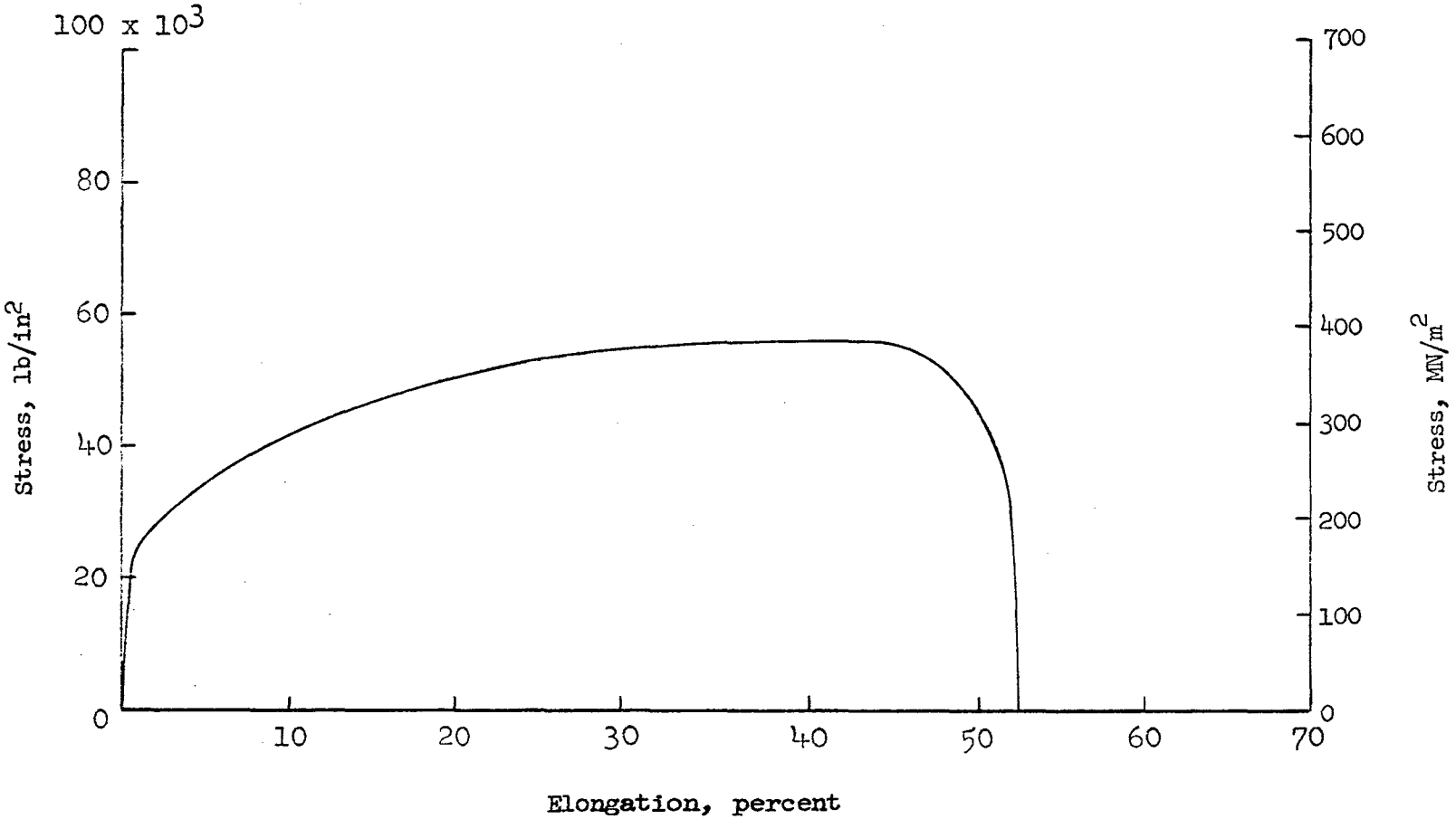

Figure 11.- Stress-strain characteristics of low-carbon nickel metal used as horizontal-strain straps on configuration 2.

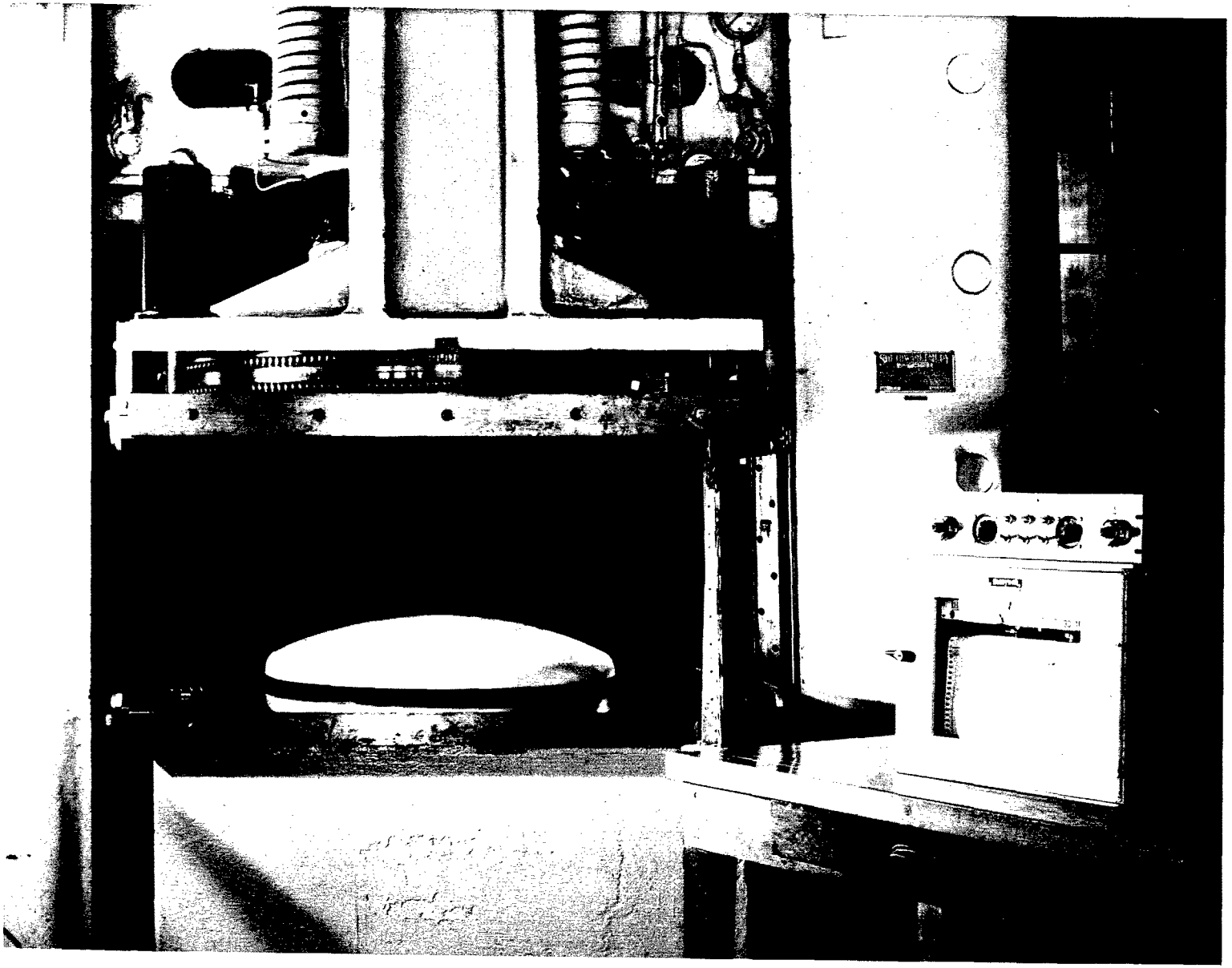

Figure 12.- Setup used to obtain heat-shield stiffness.

L-63-6075

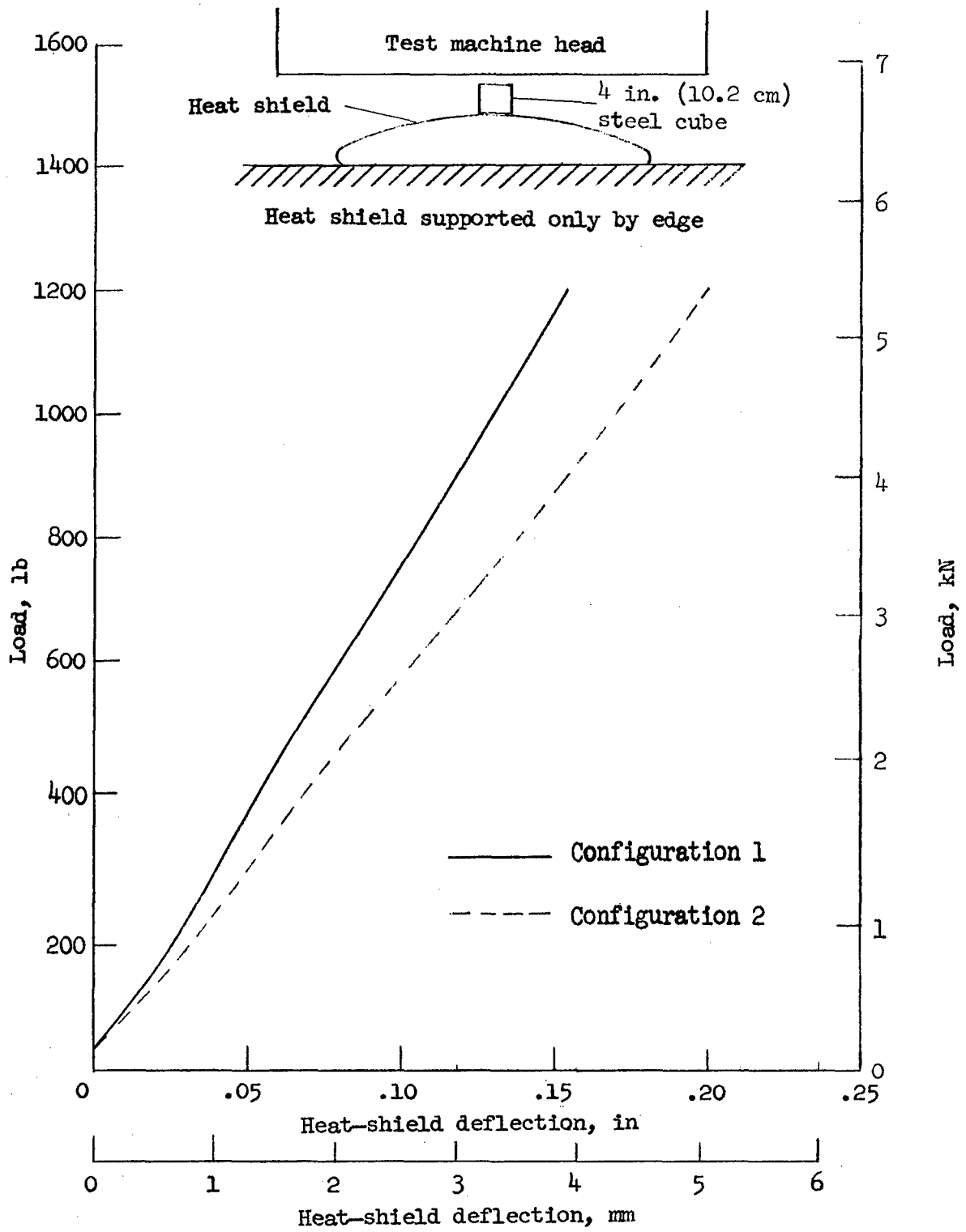

Figure 13.- Force-deflection characteristics for heat shields used on configurations 1 and 2. All values are model scale.

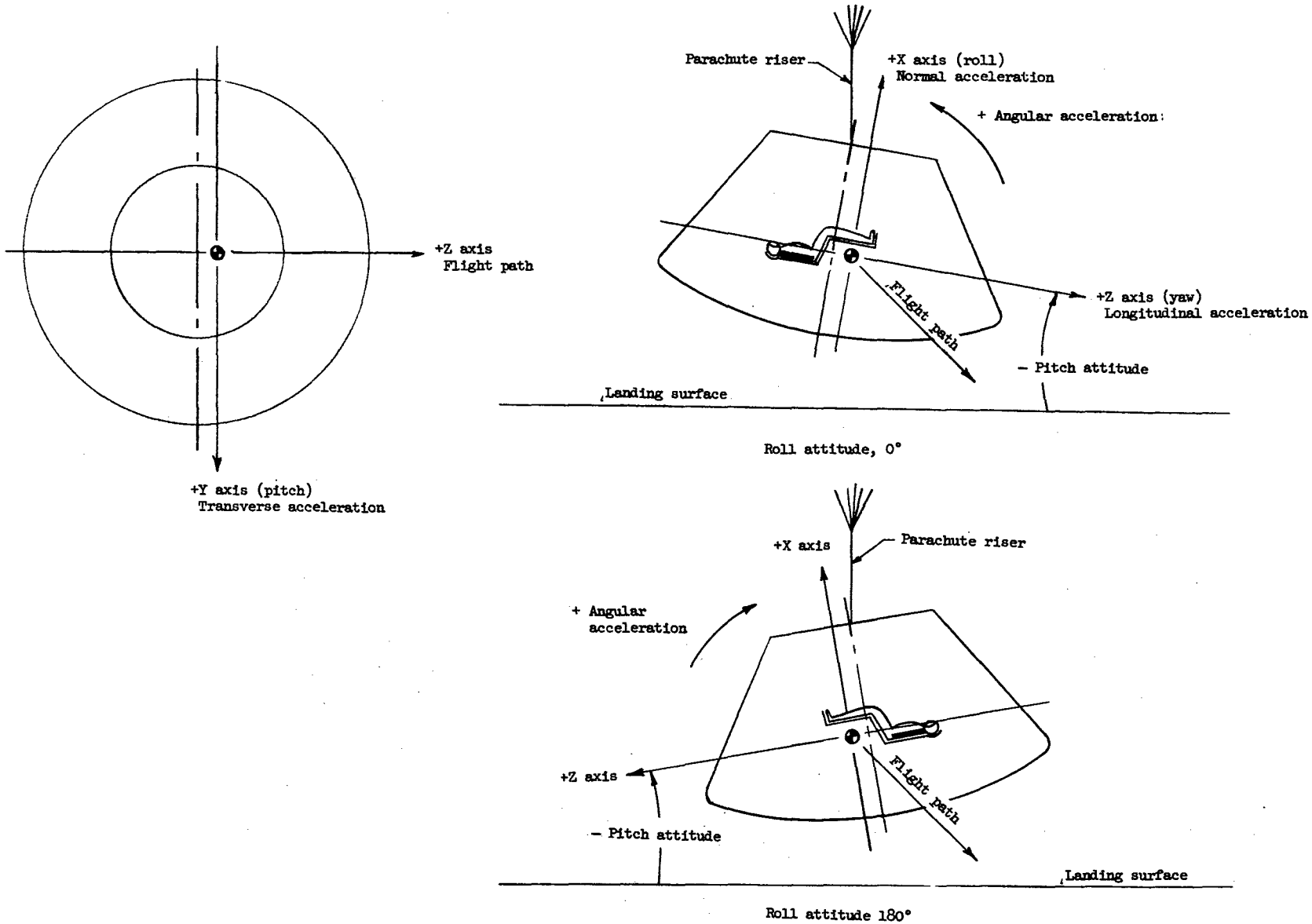

Figure 14.- Sketches identifying acceleration axes, attitudes, force directions, and flight path.

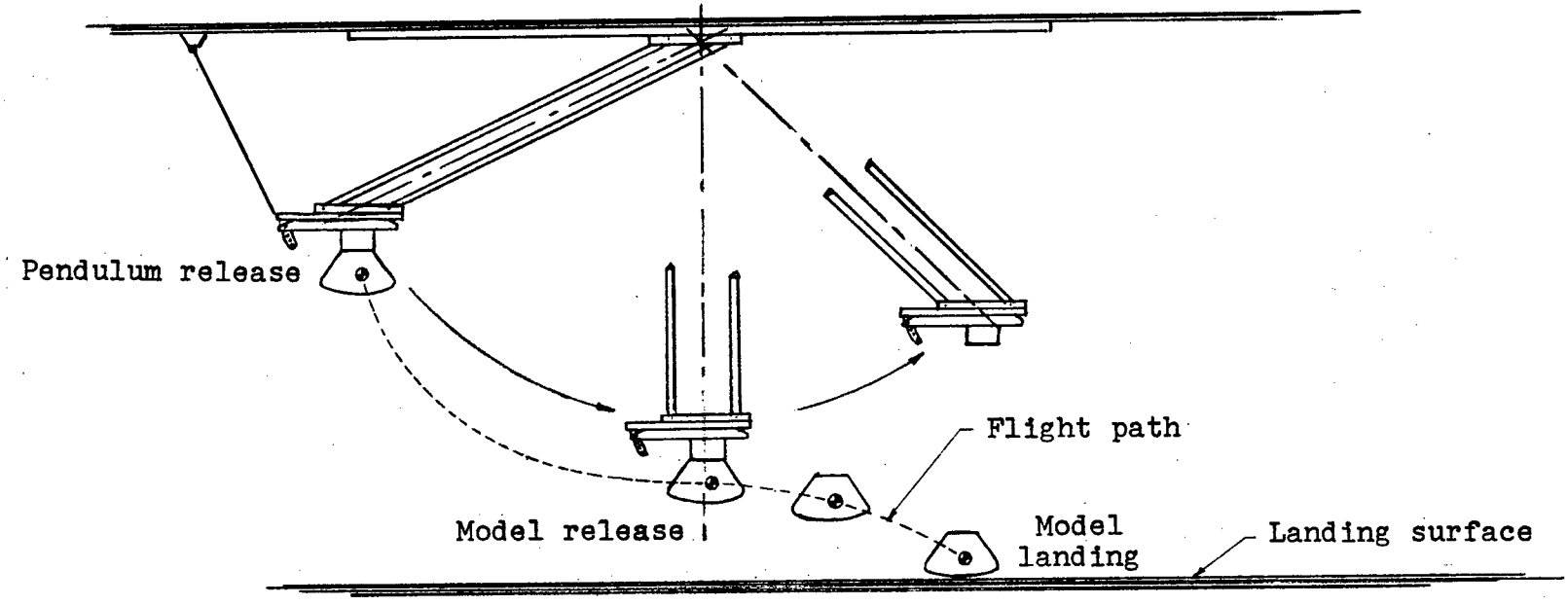

Figure 15.- Sketch showing pendulum operation during model launch and landing.

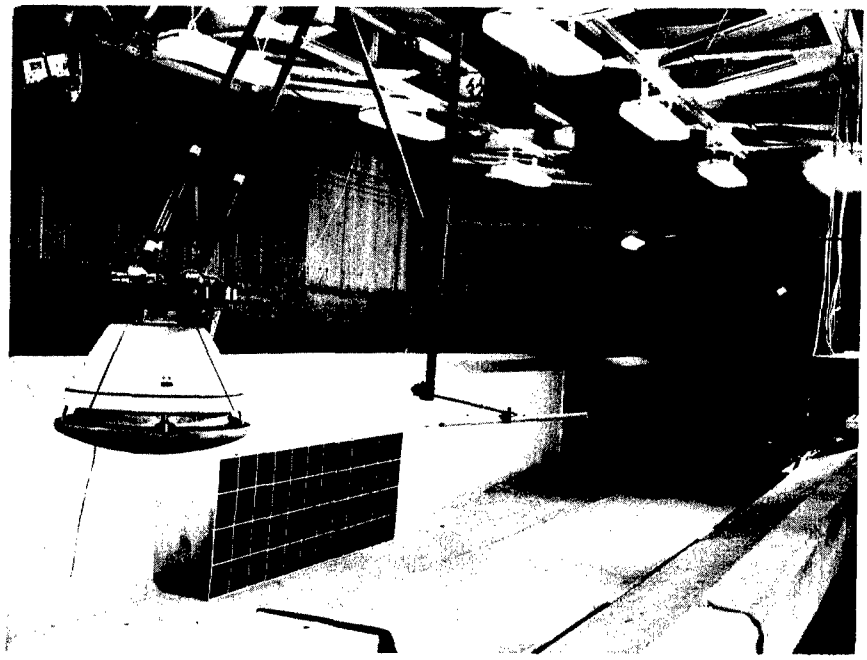

(a) Hard surface landings. L-63-1692

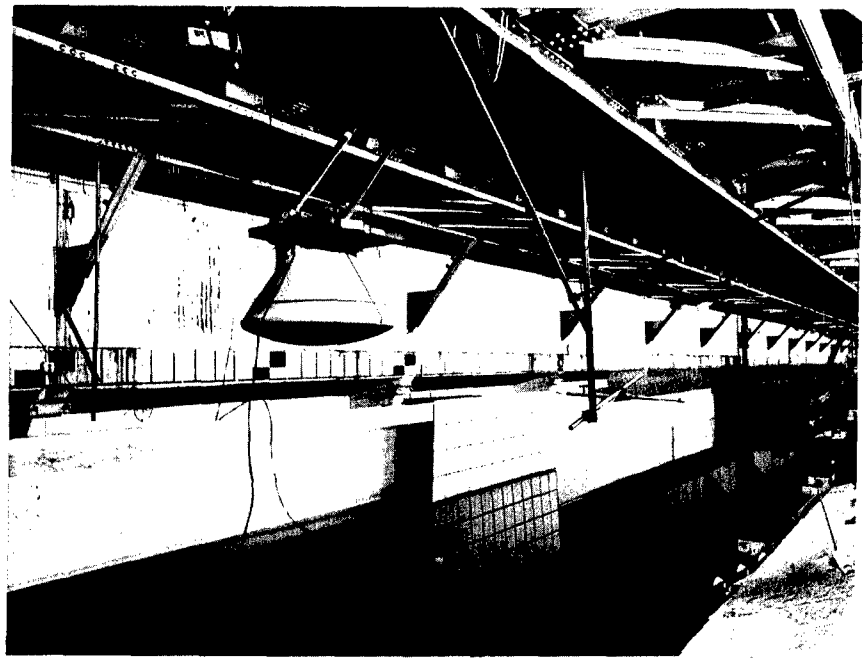

(b) Calm water landings. L-63-6192

Figure 16.- Test area setup showing model on carriage in pulled back position.

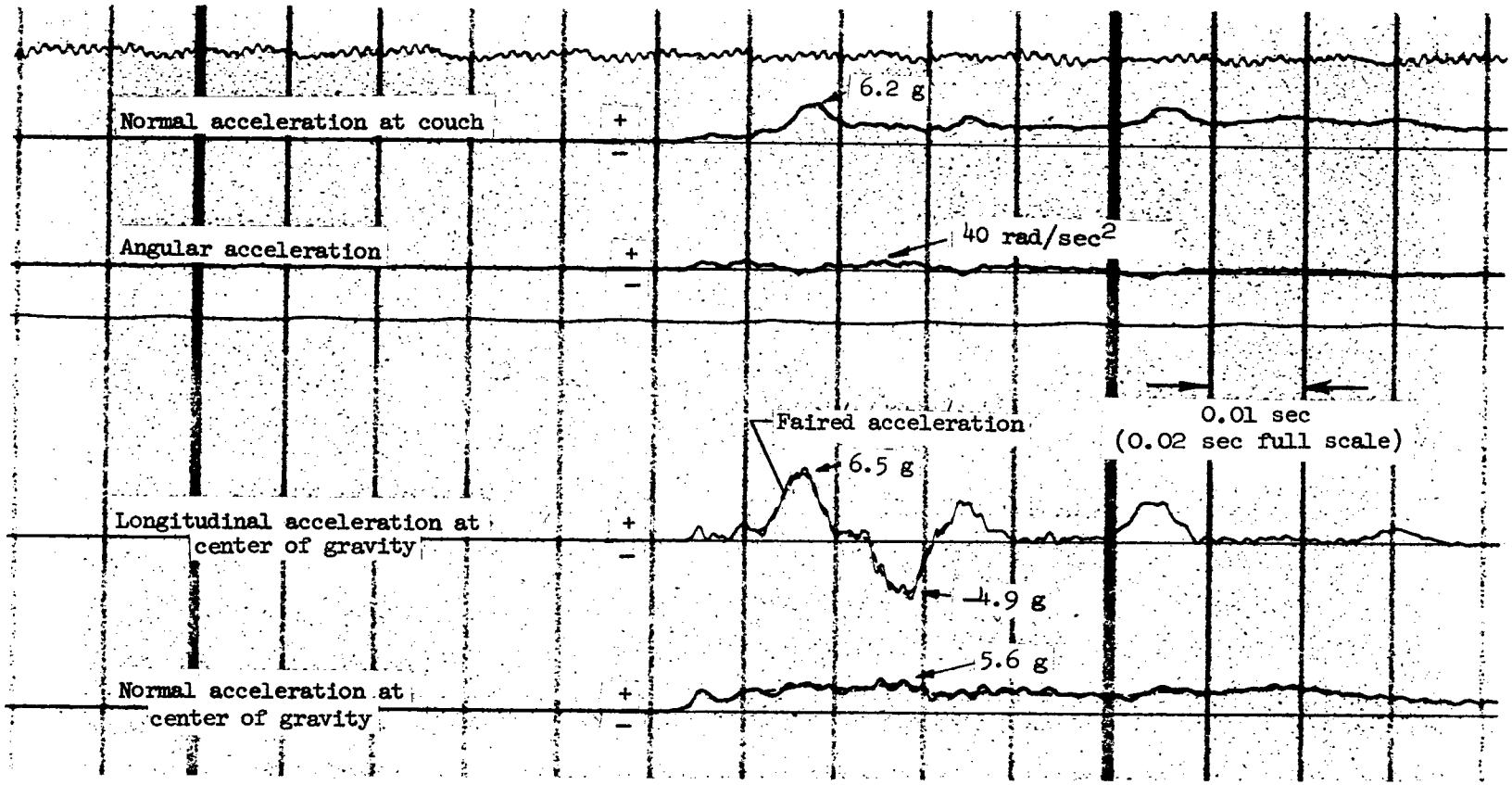

(a) Water landing surface, vertical velocity, 23 ft/sec (7.0 m/s).

Figure 17.- Typical oscillograph records of accelerations for configuration 1. Nominal landing attitude, -10° pitch; horizontal velocity, 30 ft/sec (9.1 m/s); roll attitude, 0°. All values are full scale.

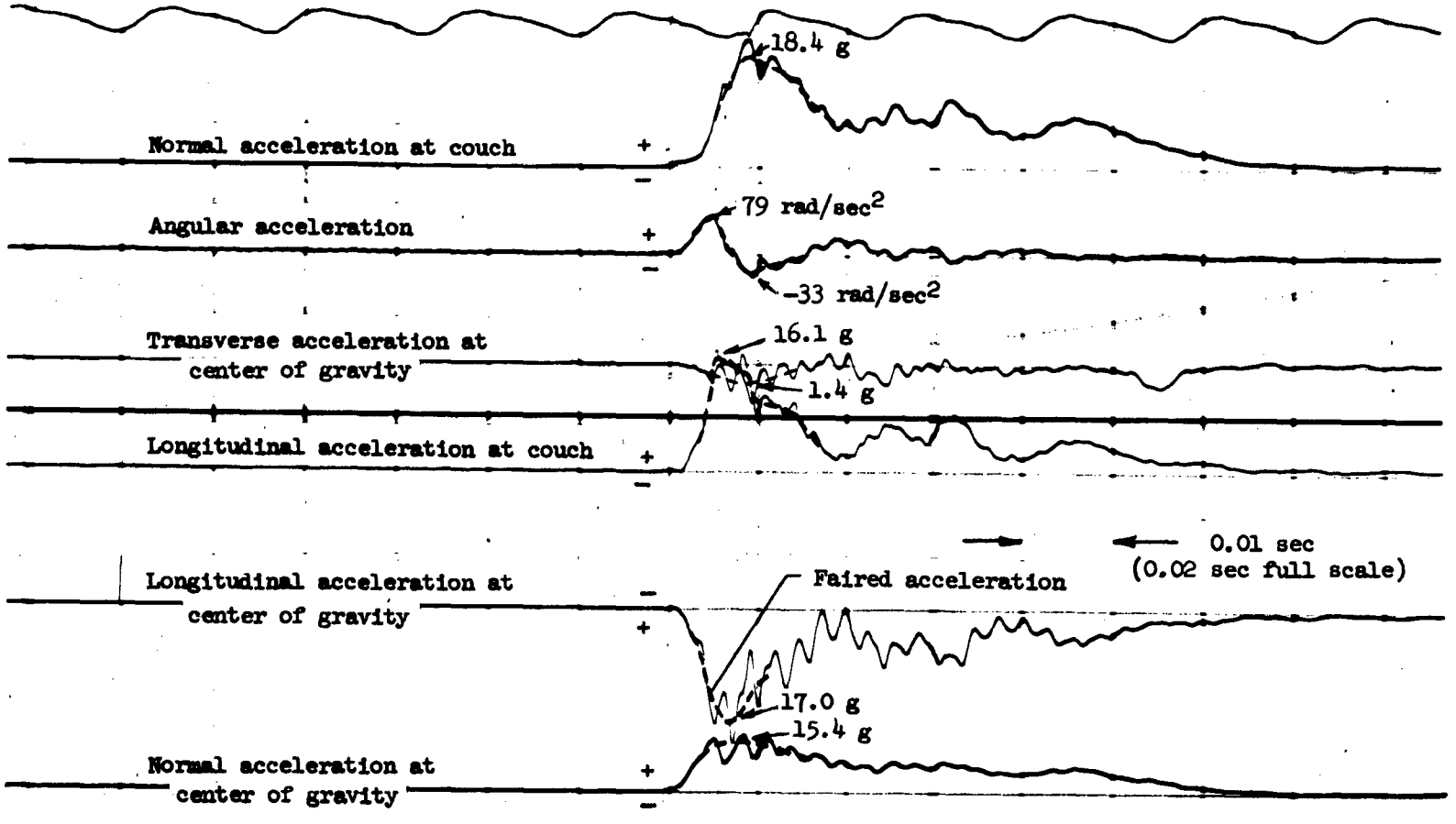

(b) Sand landing surface; vertical velocity, 30 ft/sec (9.1 m/s).

Figure 17.- Continued.

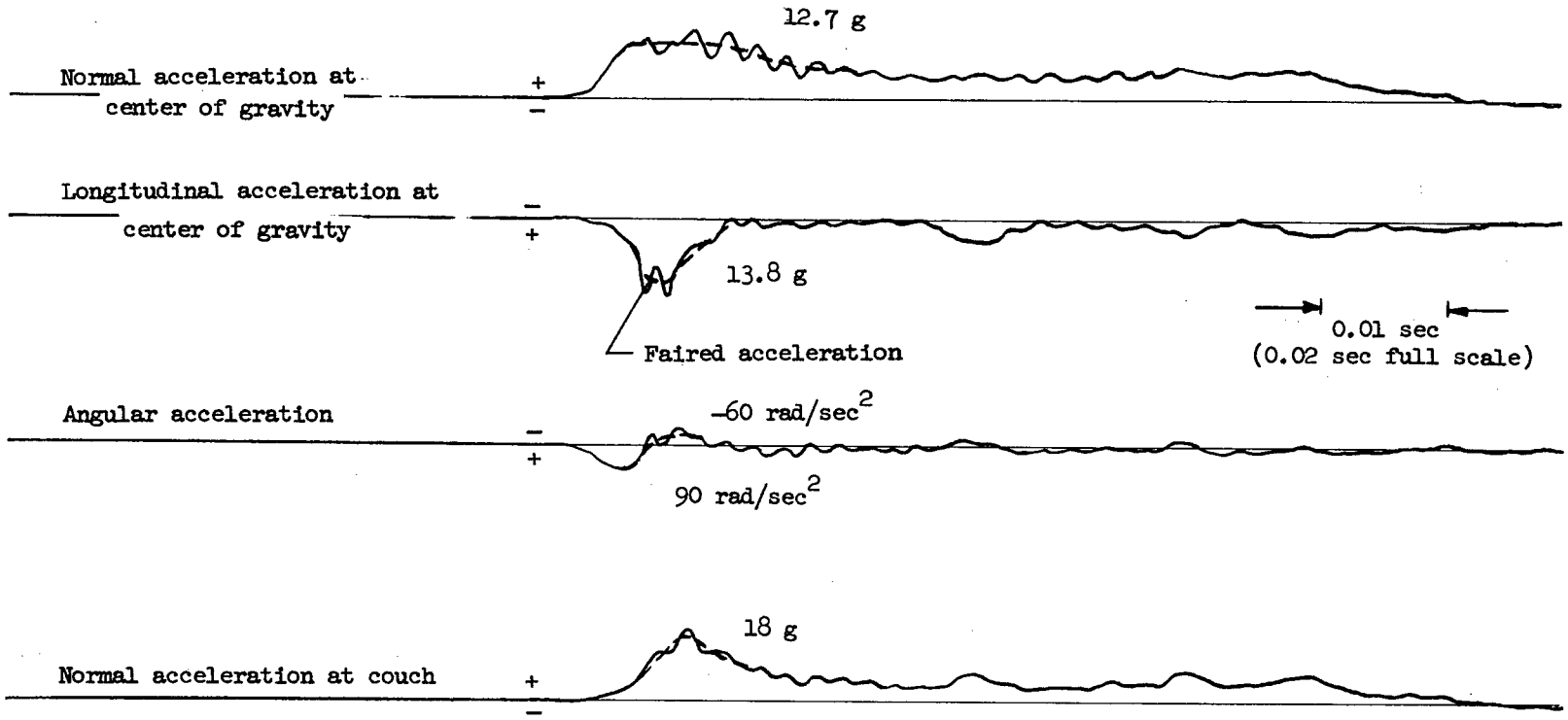

(c) Clay-gravel composite landing surface; vertical velocity, 23 ft/sec (7.0 m/s).

Figure 17.- Concluded.

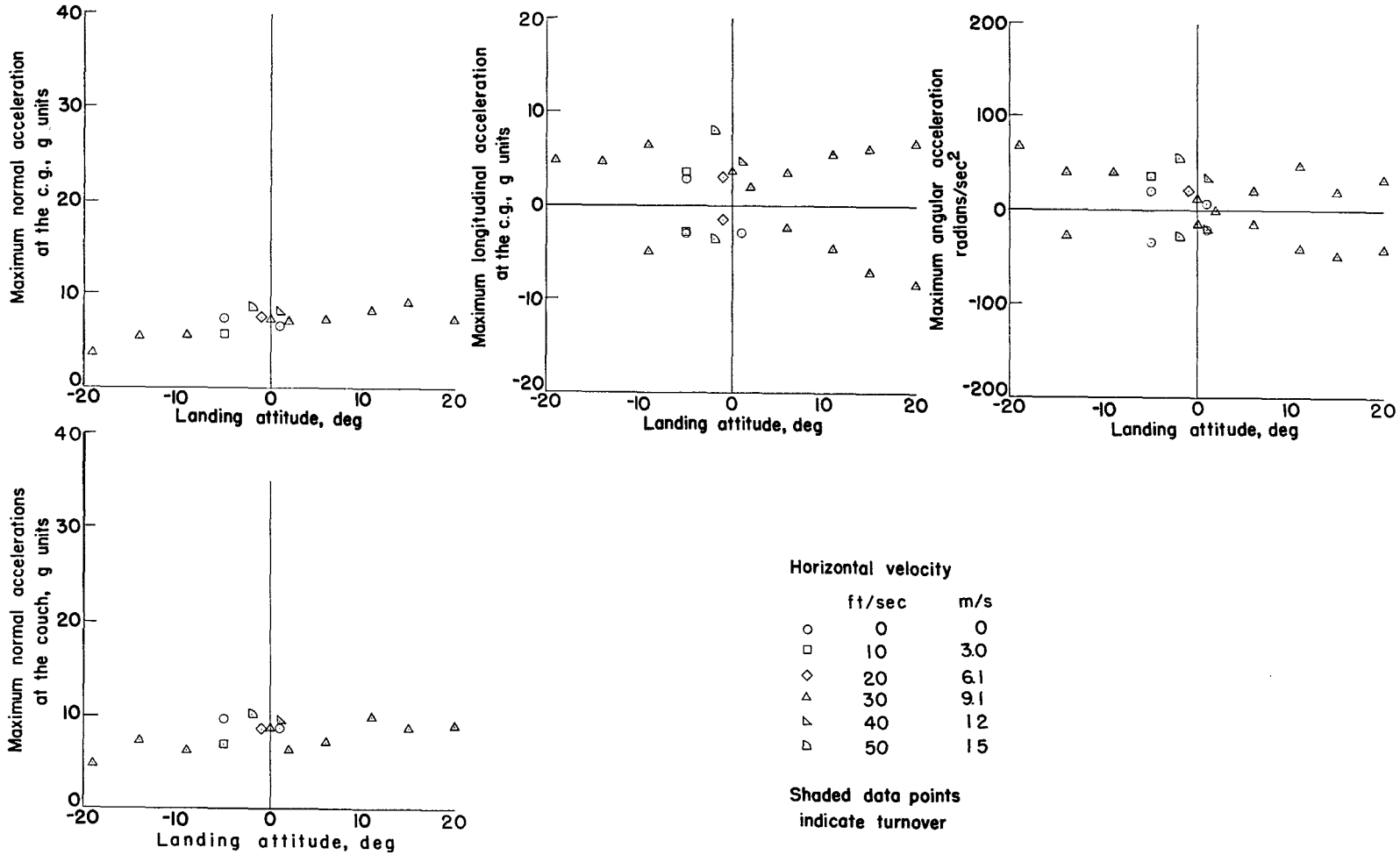

(a) Water landing surface. Vertical velocity, 23 ft/sec (7.0 m/s); roll attitude, 0^{o}.

Figure 18.- Maximum accelerations for configuration 1.

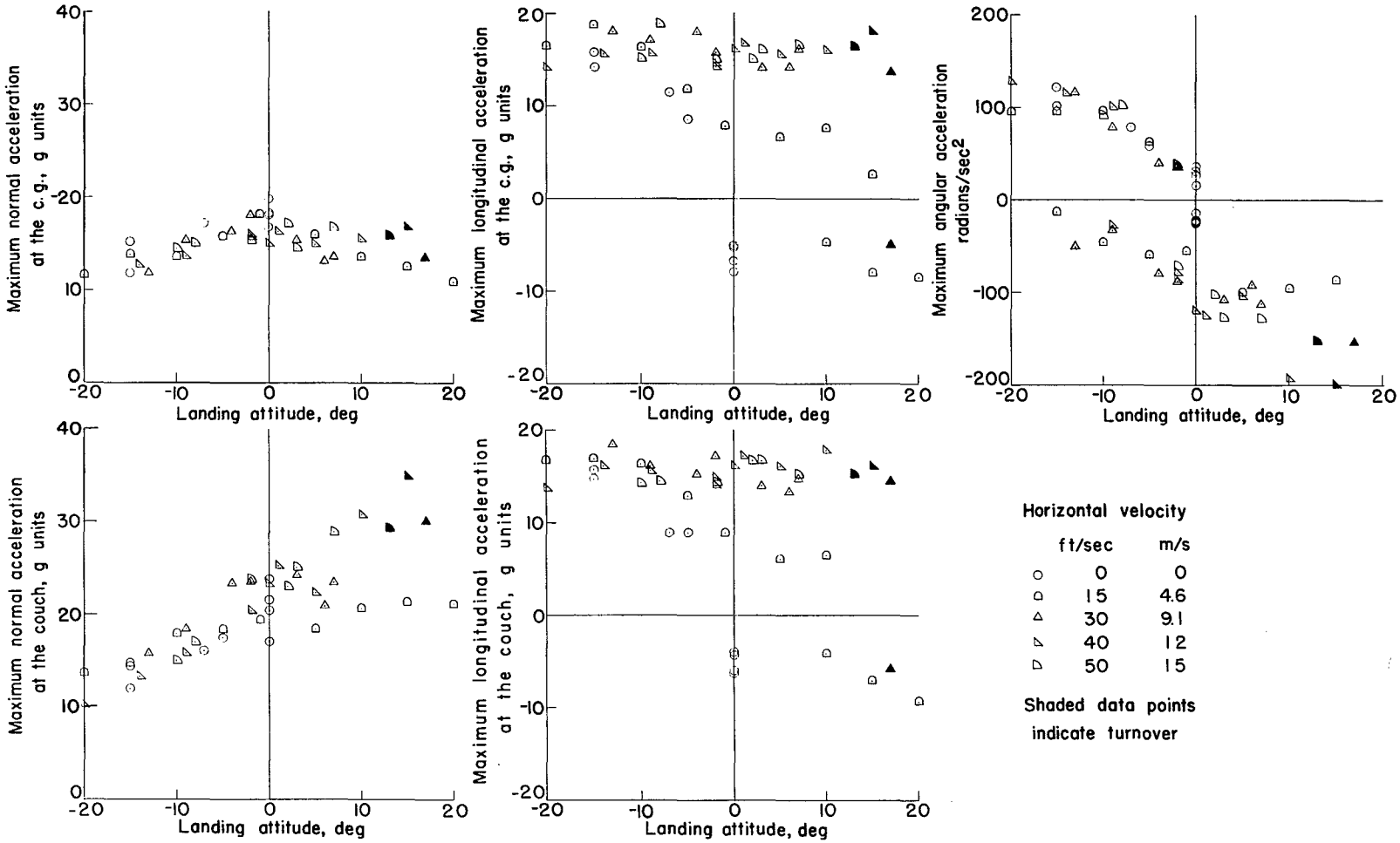

(b) Sand landing surface. Vertical velocity, 30 ft/sec (9.1 m/s); roll attitude, 0^0.

Figure 18.- Continued.

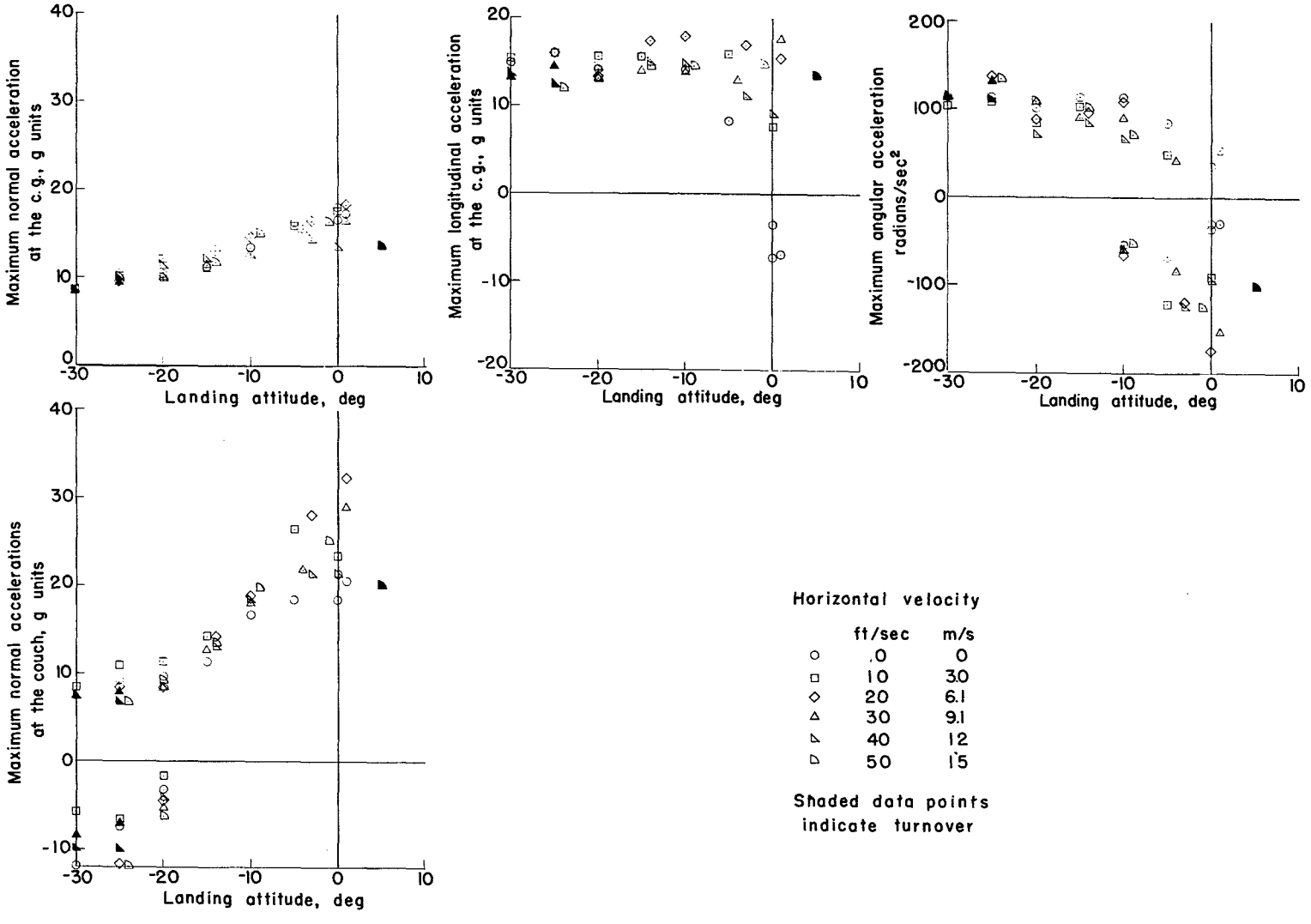

(c) Clay-gravel composite landing surface. Vertical velocity, 23 ft/sec (7.0 m/s); roll attitude, 0^0.

Figure 18.- Concluded.

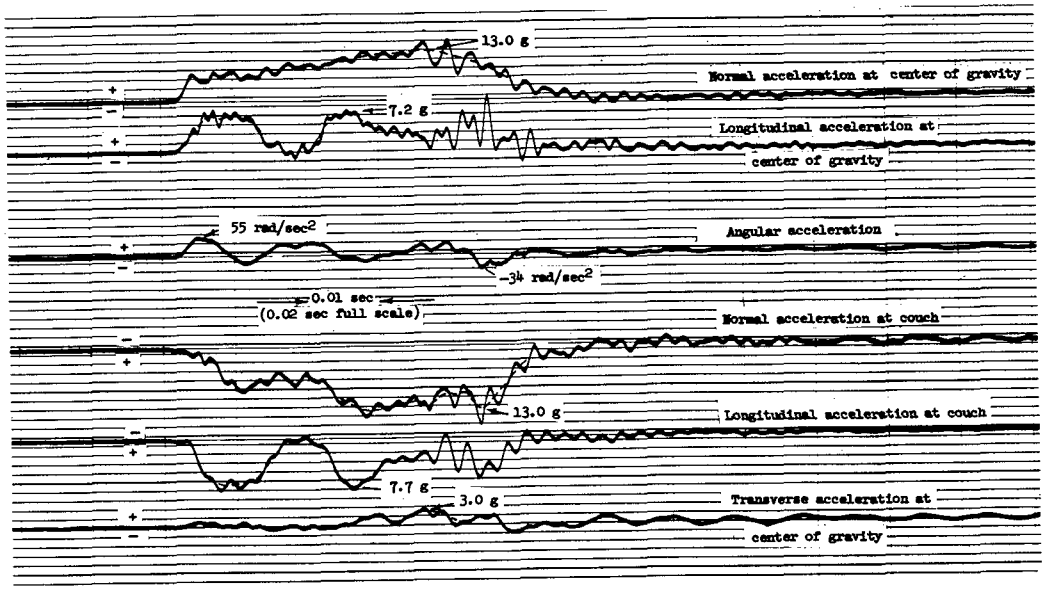

(a) Landing attitude, -11°.

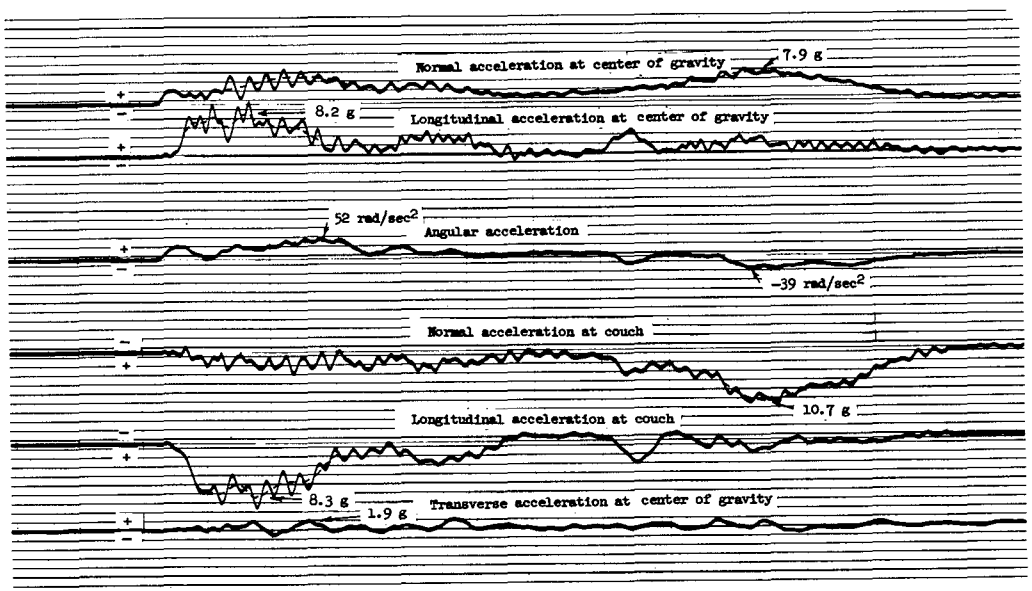

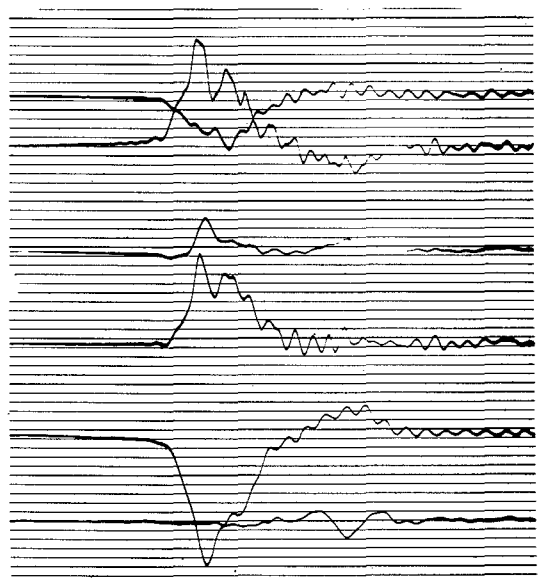

Accelerations during turnover

(b) Landing attitude, -27°.

Figure 19.- Typical oscillograph records of accelerations for configuration 2 landed on a hard clay-gravel composite surface. Vertical velocity, 23 ft/sec (7.0 m/s); horizontal velocity, 30 ft/sec (9.1 m/sec); roll attitude, 0°. All values are full scale.

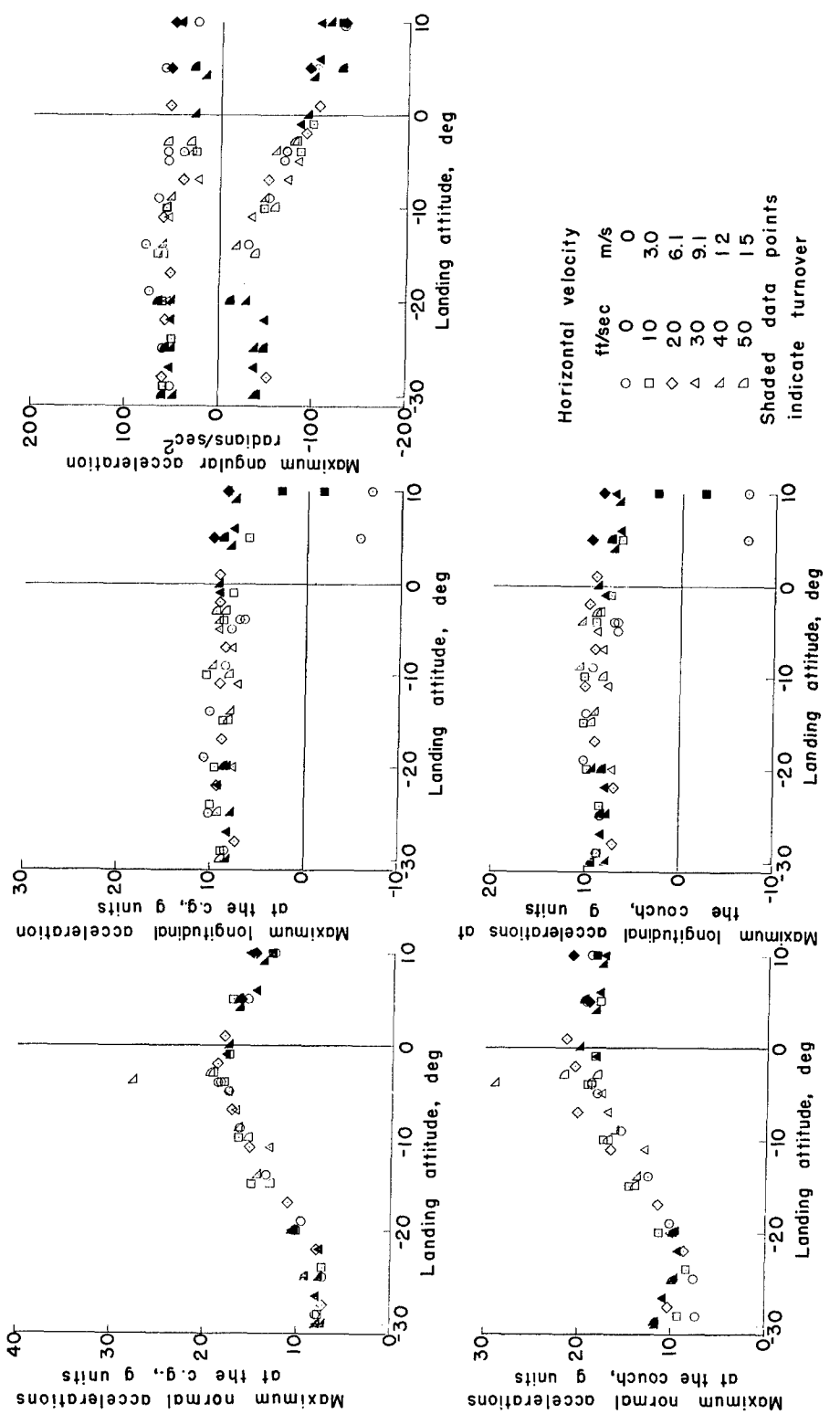

Figure 20.- Maximum accelerations for configuration 2 landed on a hard clay-gravel composite surface. Vertical velocity, 23 to 25 ft/sec (7.0 to 7.6 m/s); roll attitude, 0^0.

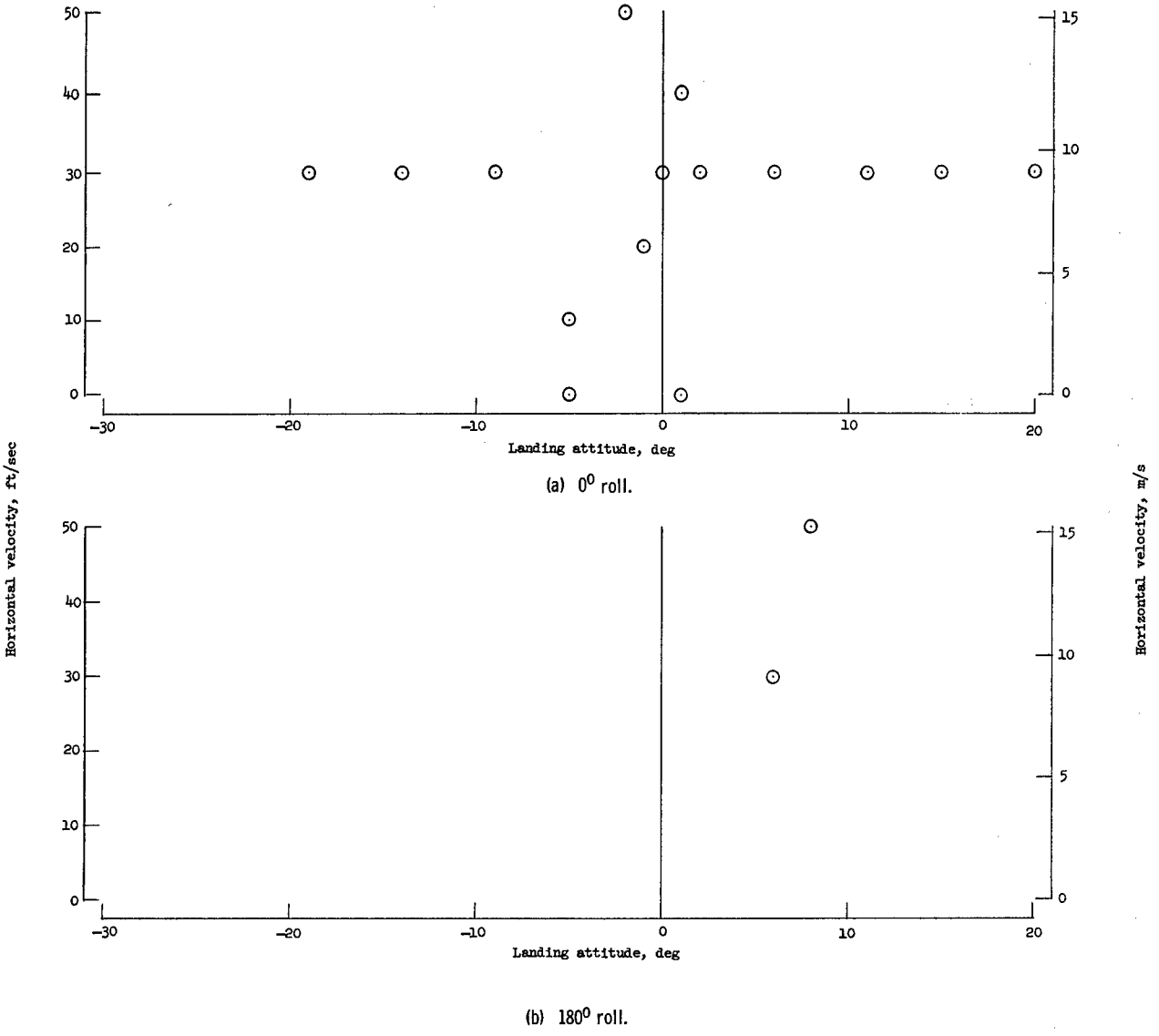

(a) 0^0 roll.

(b) 180^0 roll.

Figure 21.- Stability characteristics for configuration 1 landed on calm water. Vertical velocity, 23 ft/sec (7.0 m/s). All values are full scale.

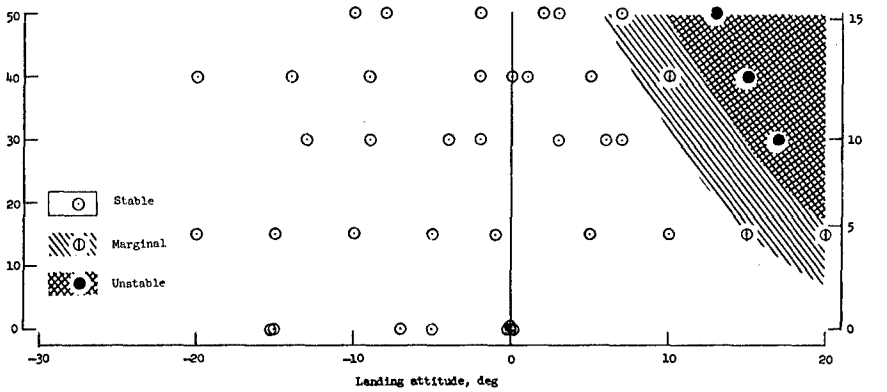

(a) 0^0 roll.

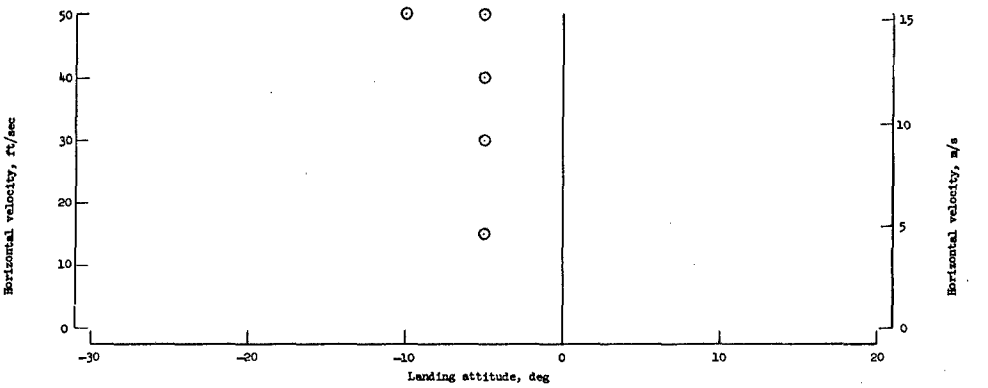

(b) 90^0 roll.

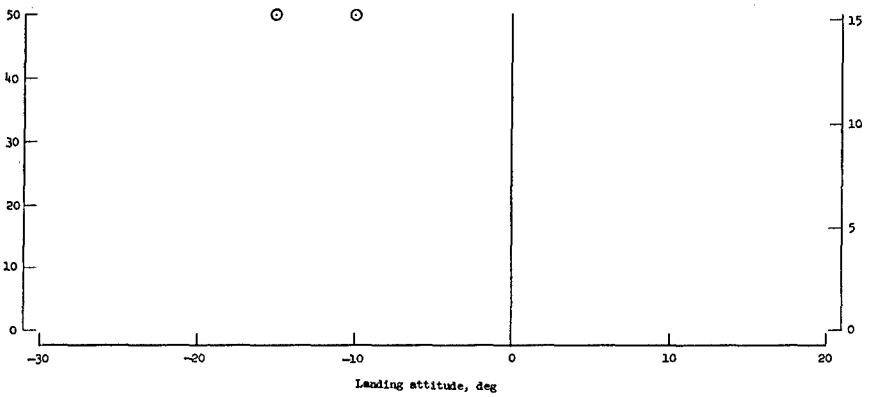

(c) 180^0 roll.

Figure 22.- Stability characteristics for configuration 1 landed on a dry sand landing surface. Vertical velocity, 30 ft/sec (9.1 m/s). All values are full scale.

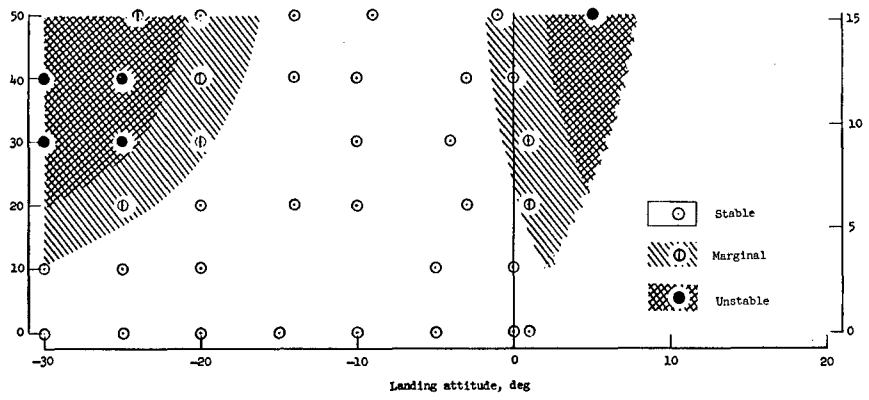

(a) 0^0 roll.

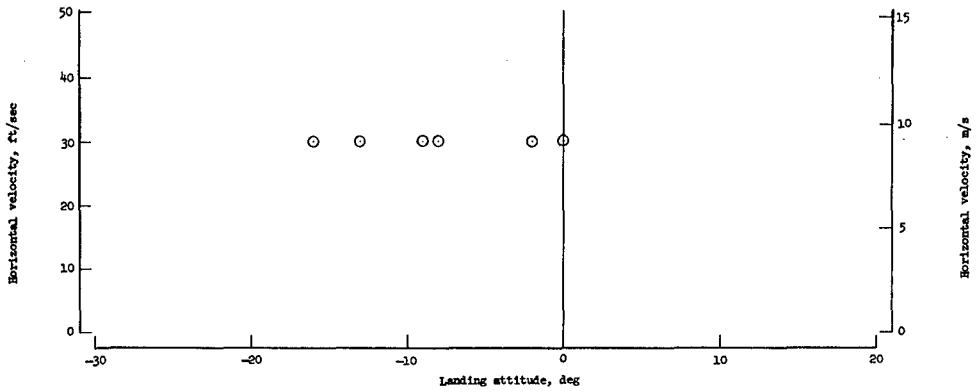

(b) 90^0 roll.

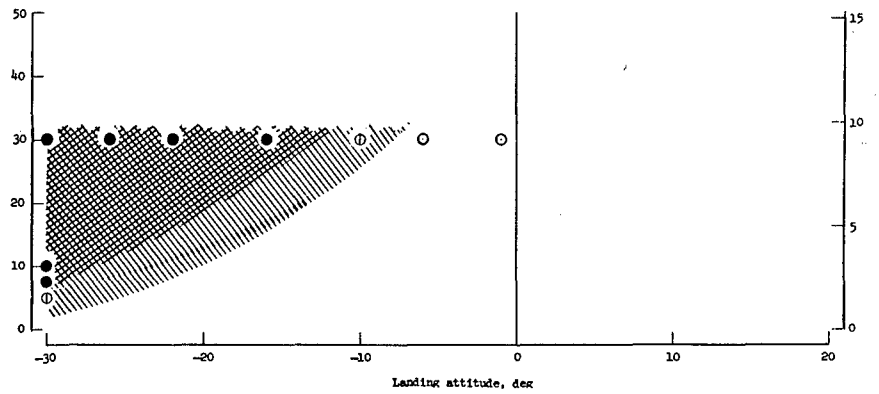

(c) 180^0 roll.

Figure 23.- Stability characteristics for configuration 1 landed on a hard clay-gravel composite surface. Vertical velocity, 23 ft/sec (7.0 m/s). All values are full scale.

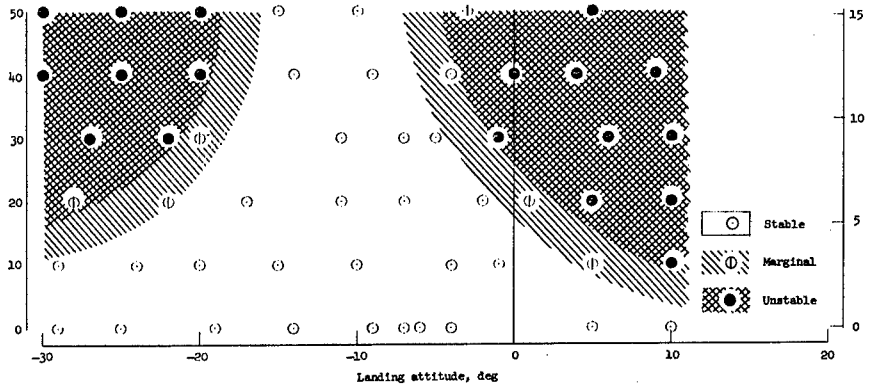

(a) 0^0 roll.

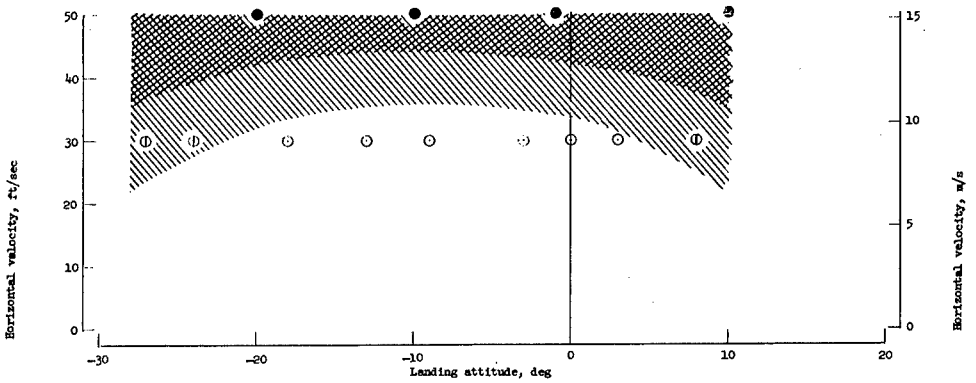

(b) 90^0 roll.

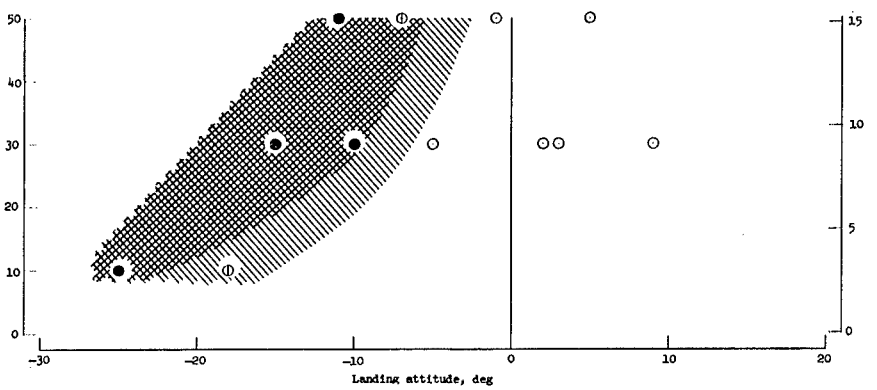

(c) 180^0 roll.

Figure 24.- Stability characteristics for configuration 2 landed on a hard clay-gravel composite surface. Vertical velocity, 23 to 25 ft/sec (7.0 to 7.6 m/s). All values are full scale.

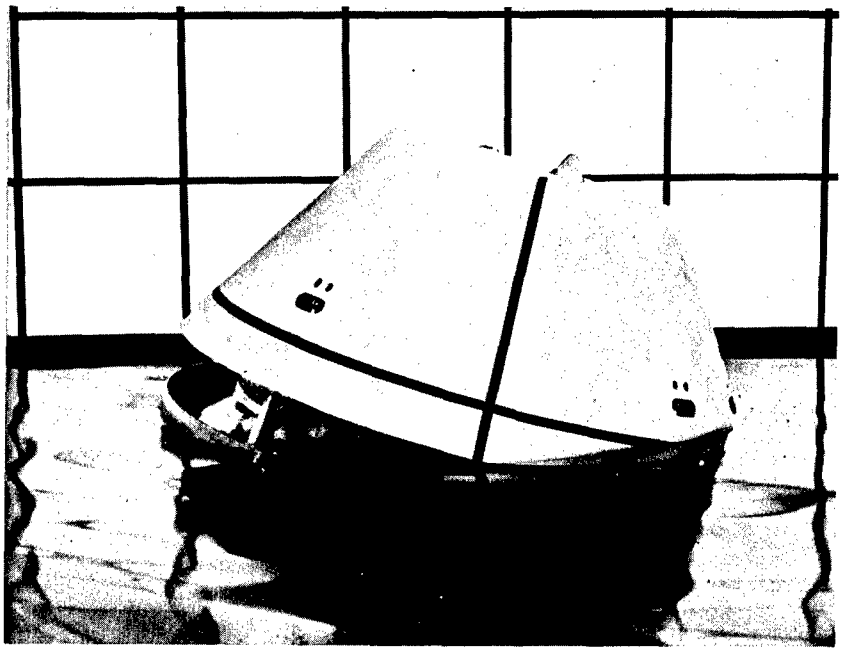

(a) Stable position floating upright.

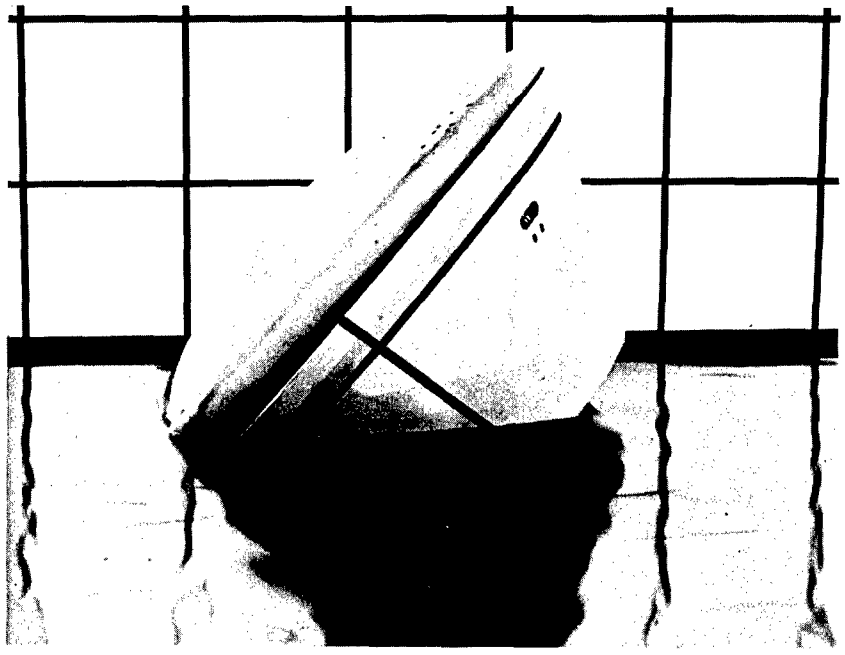

(b) Stable position after turnover.

Figure 25.- Photographs of configuration 1 floating in calm water. L-65-7913

A motion-picture film supplement L-886 is available on loan. Requests will be filled in the order received. You will be notified of the approximate date scheduled.

The film (16 mm, color, silent) shows landing tests of the 1/4-scale model of the Apollo command module made on water, sand, and the hard clay-gravel composite landing surfaces.

Requests for the film should be addressed to:

Chief, Photographic Division
NASA Langley Research Center
Langley Station
Hampton, Va. 23365

CUT

Date _____

Please send, on loan, copy of film supplement L-886 to TN D-3059

_____
Name of organization

_____
Street number

_____
City and State Zip code

Attention: Mr. _____

Title _____